IEC 61280-1-4

Edition 3.0   2023-01
REDLINE VERSION

INTERNATIONAL
STANDARD

colour
inside

**Fibre optic communication subsystem test procedures –
Part 1-4: General communication subsystems – Light source encircled flux
measurement method**

About the IEC
The International Electrotechnical Commission (IEC) is the leading global organization that prepares and publishes International Standards for all electrical, electronic and related technologies.

About IEC publications
The technical content of IEC publications is kept under constant review by the IEC. Please make sure that you have the latest edition, a corrigendum or an amendment might have been published.

IEC publications search - webstore.iec.ch/advsearchform
The advanced search enables to find IEC publications by a variety of criteria (reference number, text, technical committee, …). It also gives information on projects, replaced and withdrawn publications.

IEC Just Published - webstore.iec.ch/justpublished
Stay up to date on all new IEC publications. Just Published details all new publications released. Available online and once a month by email.

IEC Customer Service Centre - webstore.iec.ch/csc
If you wish to give us your feedback on this publication or need further assistance, please contact the Customer Service Centre: sales@iec.ch.

IEC Products & Services Portal - products.iec.ch
Discover our powerful search engine and read freely all the publications previews. With a subscription you will always have access to up to date content tailored to your needs.

Electropedia - www.electropedia.org
The world's leading online dictionary on electrotechnology, containing more than 22 300 terminological entries in English and French, with equivalent terms in 19 additional languages. Also known as the International Electrotechnical Vocabulary (IEV) online.

IEC 61280-1-4

Edition 3.0   2023-01
REDLINE VERSION

INTERNATIONAL STANDARD

colour inside

Fibre optic communication subsystem test procedures –
Part 1-4: General communication subsystems – Light source encircled flux measurement method

INTERNATIONAL
ELECTROTECHNICAL
COMMISSION

ICS 33.180.01

ISBN 978-2-8322-6399-0

Warning! Make sure that you obtained this publication from an authorized distributor.

CONTENTS

INTERNATIONAL ELECTROTECHNICAL COMMISSION

_____

FIBRE OPTIC COMMUNICATION SUBSYSTEM TEST PROCEDURES –

Part 1-4: General communication subsystems – Light source encircled flux measurement method

FOREWORD

1) The International Electrotechnical Commission (IEC) is a worldwide organization for standardization comprising all national electrotechnical committees (IEC National Committees). The object of IEC is to promote international co-operation on all questions concerning standardization in the electrical and electronic fields. To this end and in addition to other activities, IEC publishes International Standards, Technical Specifications, Technical Reports, Publicly Available Specifications (PAS) and Guides (hereafter referred to as "IEC Publication(s)"). Their preparation is entrusted to technical committees; any IEC National Committee interested in the subject dealt with may participate in this preparatory work. International, governmental and non-governmental organizations liaising with the IEC also participate in this preparation. IEC collaborates closely with the International Organization for Standardization (ISO) in accordance with conditions determined by agreement between the two organizations.

2) The formal decisions or agreements of IEC on technical matters express, as nearly as possible, an international consensus of opinion on the relevant subjects since each technical committee has representation from all interested IEC National Committees.

3) IEC Publications have the form of recommendations for international use and are accepted by IEC National Committees in that sense. While all reasonable efforts are made to ensure that the technical content of IEC Publications is accurate, IEC cannot be held responsible for the way in which they are used or for any misinterpretation by any end user.

4) In order to promote international uniformity, IEC National Committees undertake to apply IEC Publications transparently to the maximum extent possible in their national and regional publications. Any divergence between any IEC Publication and the corresponding national or regional publication shall be clearly indicated in the latter.

5) IEC itself does not provide any attestation of conformity. Independent certification bodies provide conformity assessment services and, in some areas, access to IEC marks of conformity. IEC is not responsible for any services carried out by independent certification bodies.

6) All users should ensure that they have the latest edition of this publication.

7) No liability shall attach to IEC or its directors, employees, servants or agents including individual experts and members of its technical committees and IEC National Committees for any personal injury, property damage or other damage of any nature whatsoever, whether direct or indirect, or for costs (including legal fees) and expenses arising out of the publication, use of, or reliance upon, this IEC Publication or any other IEC Publications.

8) Attention is drawn to the Normative references cited in this publication. Use of the referenced publications is indispensable for the correct application of this publication.

9) Attention is drawn to the possibility that some of the elements of this IEC Publication may be the subject of patent rights. IEC shall not be held responsible for identifying any or all such patent rights.

This redline version of the official IEC Standard allows the user to identify the changes made to the previous edition IEC 61280-1-4:2009. A vertical bar appears in the margin wherever a change has been made. Additions are in green text, deletions are in strikethrough red text.

IEC 61280-1-4 has been prepared by subcommittee 86C: Fibre optic systems and active devices, of IEC technical committee 86: Fibre optics. It is an International Standard.

This third edition cancels and replaces the second edition published in 2009. This edition constitutes a technical revision.

This edition includes the following significant technical changes with respect to the previous edition:

a) improvement of calibration procedure and calibration traceability;
b) improvement of fibre shaker description and requirements;
c) addition of pulsed light sources;
d) removal of a poorly traceable calibration process using a micro positioner.

The text of this International Standard is based on the following documents:

Draft	Report on voting
86C/1806/CDV	86C/1828/RVC

Full information on the voting for its approval can be found in the report on voting indicated in the above table.

The language used for the development of this International Standard is English.

This document was drafted in accordance with ISO/IEC Directives, Part 2, and developed in accordance with ISO/IEC Directives, Part 1 and ISO/IEC Directives, IEC Supplement, available at www.iec.ch/members_experts/refdocs. The main document types developed by IEC are described in greater detail at www.iec.ch/publications.

A list of all parts of the IEC 61280 series can be found, under the general title *Fibre optic communication subsystem test procedures*, on the IEC website.

The committee has decided that the contents of this document will remain unchanged until the stability date indicated on the IEC website under webstore.iec.ch in the data related to the specific document. At this date, the document will be

• reconfirmed,
• withdrawn,
• replaced by a revised edition, or
• amended.

IMPORTANT – The "colour inside" logo on the cover page of this document indicates that it contains colours which are considered to be useful for the correct understanding of its contents. Users should therefore print this document using a colour printer.

INTRODUCTION

0.1   ~~General~~

This part of IEC 61280 ~~is used~~ specifies how to measure the encircled flux of a multimode light source. Encircled flux is a ~~measure, as a function of radius, of the~~ fraction of the cumulative output power to the total output power ~~radiating from~~ as a function of radial distance from the centre of the multimode optical fibre's core.

The basic approach is to collect two-dimensional (2D) nearfield data, using a calibrated camera, and to mathematically convert the 2D data into three normalized functions of radial distance from the fibre's optical centre. The three functions are intensity, incremental flux, and encircled flux. ~~Intensity has dimension optical power per area; incremental flux has dimension power per differential of radius; and encircled flux has dimension total optical power, all three being functions of radius.~~ The intensity represents optical power per surface area (in watts per square meter). The incremental flux represents optical power per radius differential (in watts per meter), and the encircled flux represents a fraction of the cumulative output power to the total output power.

These three radial functions are intended to characterize fibre optic laser sources either for use in mathematical models predicting the minimum guaranteed length of a communications link, or to qualify a light source to measure insertion loss in multimode links.

0.2   ~~Changes from previous edition~~

~~This edition of the standard differs from its predecessor in both scope and content. Many of the content changes improve the measurement precision. Several changes have been made to the computation procedure:~~

- ~~the integration methodology of the radial functions was simple summation, and is now specified to use trapezoidal integration or other higher-order techniques (see 9.3);~~
- ~~a baseline subtraction step is specified to improve immunity to DC drifts (see 9.2.2 and 9.2.3);~~
- ~~the ring width parameter is explicitly specified (see 9.2.1);~~
- ~~the integration limit is specified (see 9.3).~~

~~The geometric calibration of the apparatus microscope now specifies either (depending on the application) the methodology of IEC 61745 or the original technique using the micropositioning stage (see Clause 7). Pixel sensitivity uniformity correction is now optional.~~

0.3   ~~Assumptions applicable to the characterization of data sources~~

~~The 50-μm or 62,5-μm core near-parabolic graded-index multimode fibre used as the "test jumper assembly" is treated as if it possessed perfect circular symmetry about its optical centre, as asymmetries in the launched optical flux distributions will dominate any lopsidedness of the test jumper assembly. It is further assumed that all cladding modes will be stripped by passage through the specified ten metres or more of fibre. The modes of a mode group need not carry equal flux. (In fact, with such short fibres, one thousand metres or less, unequal distribution of flux in the modes of a group is the norm, not the exception.)~~

0.4   ~~Assumptions applicable to the characterization of measurement sources~~

~~Measurement sources are assumed to be sufficiently broadband and incoherent that speckle is not a problem, and to have a sufficiently symmetrical nearfield distribution that the truncated centroid of that nearfield indicates the location of the optical centre of the fibre with sufficient accuracy for the purposes of this standard.~~

**FIBRE OPTIC COMMUNICATION SUBSYSTEM
TEST PROCEDURES –**

**Part 1-4: General communication subsystems –
Light source encircled flux measurement method**

1 Scope

~~This part of IEC 61280 is intended to characterize the encircled flux of two types of light sources: transmission light sources, which are usually coherent and substantially under-excite the mode volume of a multimode fibre, and measurement light sources, which are incoherent and excite most of the mode volume of a multimode fibre.~~

This part of IEC 61280 establishes the characterization process of the encircled flux measurement method of light sources intended to be used with multimode fibre.

This document sets forth a ~~standard~~ procedure for the collection of two-dimensional fibre optic nearfield greyscale data and subsequent reduction to one-dimensional data expressed as a set of three sampled parametric functions of radius from the fibre's optical centre. ~~This revision of IEC 61280-1-4 continues to fulfil its original purpose, characterization of transmission light sources, which enables the accurate mathematical prediction of minimum guaranteed link length in 1 gigabit per second or greater fibre optic data communication systems. New to this revision is support for improved measurement precision of insertion loss in multimode fibre optic links through the characterization of measurement light sources.~~

Estimation of the fibre core diameter is not an objective of this document.

2 Normative references

The following documents are referred to in the text in such a way that some or all of their content constitutes requirements of this document. For dated references, only the edition cited applies. For undated references, the latest edition of the referenced document (including any amendments) applies.

IEC 60793-2-10, *Optical fibres – Part 2-10: Product specifications – Sectional specification for category A1 multimode fibres*

IEC 60825-1, *Safety of laser products – Part 1: Equipment classification and requirements*

~~IEC 61745:1988, *End-face image analysis procedure for the calibration of optical fibre geometry test sets*~~

3 Terms and definitions

For the purposes of this document, the following terms and definitions apply.

ISO and IEC maintain terminology databases for use in standardization at the following addresses:

- IEC Electropedia: available at https://www.electropedia.org/
- ISO Online browsing platform: available at https://www.iso.org/obp

3.1
calibration light source
light source used to find the optical centre of a multimode fibre

3.2
centroid image
image used to determine the optical centre of the multimode fibre core

3.3
corrected image
image which has had a dark image subtracted from it and whose elements have had uniformity correction applied

3.4
dark image
image taken with the measured light source either turned off or not installed in the input port

Note 1 to entry: Stray light and electrical signals of the detection system will remain in the dark image.

3.5
image
two-dimensional rectangular array of numbers whose elements are pixels and whose pixel values linearly correspond to the optical power falling on the pixels

3.6
light source
something that emits light that is coupled into a fibre, the output of which can be measured

EXAMPLE   Calibration light source, transmission light source, light source used for attenuation measurements.

3.7
measurement light source
light source intended to be used in the measurement of attenuation

3.8
nominal core radius
half the nominal core diameter of the multimode fibre to be measured

3.9
ring smoothing
technique to reduce the two dimensional near field image into a 1-D near field intensity profile while cancelling the effects of the periodic spacing of imager pixels of finite area

3.10
transmission light source
light source used to transmit digital data over multimode fibre optic links

3.11
uniformity correction
process to correct the sensitivity of a pixel so that it performs substantially like an average pixel

3.12
valid pixel
optical detection element in the detector matrix whose sensitivity, when corrected, is within 5 % of the mean sensitivity of the average conversion efficiency of the detector

4   Symbols

B baseline intensity

> NOTE 1   This value is determined from a region of the computed near field just outside the core boundary.

D distance from the centre of the centroid image to the nearest boundary of the image

D_L, D_R, D_T, D_B set of distances from the centre of the centroid image to, respectively, the left, right, top and bottom boundaries of the image

> NOTE 2   The minimum of this set is used to compute D.

$EF(i)$ encircled flux vector

$EF'(i)$ non-normalized encircled flux vector

i index parameter used in the parametric result vectors $\overline{R}(i), \overline{I}(i)$ and $EF(i)$ and $EF(i)$

I_{dark} matrix of pixel intensities of a dark image as measured by the detector and digitizer

I_{raw} matrix of pixel intensities of the light source, before correction, as measured by the detector and image digitizer

$I_{r,c}$ near-field intensity matrix

> NOTE 3   This is a matrix of pixel intensities, based on I_{raw}, as measured by the detector and corrected using U and I_{dark}.

$I(i)$ ring-smoothed intensity vector, each element being the arithmetic average of the set of radial coordinates of all the pixels in a given ring

N_R number of rings used to compute the 1-D near field

N_r number of rows in an image

> NOTE 4   All columns in an image have the same number of rows.

N_c number of columns in an image

> NOTE 5 . All rows in an image have the same number of columns.

P_{Max} most intense valid pixel in the centroid image

P_{Min} least intense valid pixel in the centroid image

R radial coordinate, in μm, of the centre of any pixel, referenced to the optical centre X_0, Y_0

$R(i)$ ring-smoothed radial vector, each element being the arithmetic average of the radii of all the pixels in the ith ring

R_{max} integration limit along the radius

S_c column-weighted summation of all pixel intensities greater than T in the centroid image

$S_I(i)$ intensity summation vector used in ring smoothing

S_P summation of all pixel intensities greater than T in the centroid image

$S_N(i)$ pixel counting vector used in ring smoothing

$S_R(i)$ radius summation vector used in ring smoothing

S_r row-weighted summation of all pixel intensities greater than T in the centroid image

S_x horizontal geometric calibration factor (along columns)

S_Y vertical geometric calibration factor (along rows)

T threshold used to determine which pixels in the centroid image will be used to determine the optical centre

> NOTE 6   All pixels greater than or equal to T are used to compute the centroid.

$U_{r,c}$ sensitivity correction matrix, applied to a dark-subtracted image to reduce non-uniformity of the detector's pixel-to-pixel conversion efficiency

W half-width, in µm, of the rings used to compute the 1-D near field

X_0 X axis (column) location of the centre of the centroid image

Y_0 Y axis (row) location of the centre of the centroid image

5   Assumptions

5.1   Assumptions applicable to the characterization of data sources

The 50 µm or 62,5 µm core near-parabolic graded-index multimode fibre used as the "test jumper assembly" is treated as if it possessed perfect circular symmetry about its optical centre, because asymmetries in the launched optical flux distributions will dominate any distortions introduced by the test jumper assembly, such as lateral and angular misalignments. It is further assumed that all cladding modes will be stripped by passage through the specified ten metres or more of fibre. The modes of a mode group need not carry equal flux. In fact, with such short fibres, one thousand metres or less, unequal distribution of flux in the modes of a group is the norm, not the exception.

5.2   Assumptions applicable to the characterization of measurement sources

Measurement sources are assumed to be sufficiently broadband and incoherent, so that speckle is not a problem, and to have a sufficiently symmetrical nearfield distribution, so that the truncated centroid of that nearfield indicates the location of the optical centre of the fibre with sufficient accuracy for the purposes of this document.

6   Apparatus

6.1   Common apparatus

6.1.1   General

Figure 1 below shows an apparatus block diagram.

IEC

a   The image digitizer ~~may~~ can be either part of a camera or a computer add-in board.

b   The detector electronics are usually integral to the camera and digitizer.

c   Attenuation is best placed in the collimating region of the optical path, but not all optical designs will have an accessible collimating region. When this is not possible, the attenuation should be placed on the detector side of the optics.

d   When a micro positioner (not shown) is employed, the input port will be physically attached to it.

Figure 1 – Apparatus block diagram

6.1.2 Computer

A computer is required, because the acquired image contains many thousands of pixels, and the reduction of the image to encircled flux requires substantial computation. The computer will usually be connected to the image digitizer to control the acquisition of an image through software and ~~may~~ can also control the micro positioner (and the source, if correlated double sampling is implemented).

6.1.3 Image digitizer

The nearfield of the fibre core is imaged onto the detector and then digitized by the image digitizer. The image digitizer ~~may~~ can be an integral part of a camera, which also contains the detector, or ~~may~~ can be an add-in frame-grabber board in the computer.

Automatic circuitry in the digitizer, for example ~~AGC or~~ automatic gain control (ABC) often found in video cameras, shall be disabled.

6.1.4 Detector

The detector is typically a charge-coupled device (CCD) or complementary metal-oxide semiconductor (CMOS) camera. Other types of array cameras ~~may~~ can be considered. In any case, detectors shall be both nominally linear and memoryless~~; this excludes for instance lead sulphide vidicon detectors~~. Absolute radiometric measurement of flux (optical power flow) is not required.

Automatic circuitry in the detector, for example ~~AGC or~~ automatic gain control often found in video cameras, shall be disabled.

The difference in conversion sensitivity from pixel to pixel in the detector will affect the measurement accuracy. The non-uniformity in the corrected conversion efficiency of the detector shall not exceed ±5 %. It is possible to calibrate and correct a detector, whose uncorrected uniformity is worse than 5 %, by applying a pixel-by-pixel sensitivity correction matrix, U, to the raw image. Often, this correction is part of the camera function (and so each element of U ~~may~~ can be taken as unity). Sometimes, the correction matrix ~~may~~ can be ~~supplied~~ provided by the detector supplier. In other cases, the correction matrix shall be determined by the procedure outlined in Clause A.2.

Detectors can have invalid pixels, which are pixels whose corrected conversion efficiency exceeds ±5 % of the average conversion efficiency of the detector. Invalid pixels will often produce no signal or, a completely saturated signal, or be stuck at some intermediate value. Detectors whose invalid pixel count exceeds 0,1 % of the total number of pixels shall be rejected.

In most cameras and image digitizers, the setting of the "black level" is user adjustable. Since the detector will be slightly noisy, it is important that the detector and digitizer do not clip random black signals at zero (in common systems, random noise in a detector will have a standard deviation less than 0,5 % of the saturation level). To ensure no clipping of the noise, when settable, set the black level to produce a small positive signal (typically at least five times the standard deviation of the noise) when no light is impinging on the detector.

6.1.5 Magnifying optics

Suitable optics shall be provided to project the magnified image of the input port onto the detector, in such a way that the detector can measure the entire nearfield flux distribution. The numerical aperture of the magnifying optics shall exceed the nominal numerical aperture of the fibres (as specified in the fibre's family specification) used in calibration or measurement. Microscope objectives are often appropriate for this purpose.

NOTE 1   When a microscope objective is used, its actual magnification as used in the present apparatus generally will not be the same as the nominal magnification factor engraved into the side of the objective, because the present apparatus differs from the standard microscope for which that nominal magnification factor was computed. The geometric calibration procedures outlined in Clause 8 determine the actual magnification.

NOTE 2   When characterizing measurement light sources, measurement precision is important, so optical distortion is kept to a minimum. Care in selection and application of the lenses and other optical components should be considered. Plan-type microscope objectives are an example of suitable optics. The procedures found in IEC 61745 can be used to assess the optical integrity of the apparatus.

NOTE 3   Reflections from optical surfaces may can seriously degrade the measurement of encircled flux. Anti-reflection coating at the wavelength of measurement or other forms of reflection control may can be considered to reduce reflections.

Measurement precision is important when characterizing measurement light sources, so that optical distortion is kept to a minimum. Careful selection and application of the lenses and other optical components is recommended. Plan-type microscope objectives are an example of suitable optics. The procedures found in IEC 61745:2017 can be used to assess the optical integrity of the apparatus.

It is important that the distance between the detector and all elements of the magnifying optics be held fixed once calibration is performed. When the relationship between these elements changes, the magnification is expected to change enough that recalibration will be required. Focusing shall be accomplished by changing only the distance between input port and the magnifying optics.

6.1.6 Attenuation Attenuator

Often, the optical flux of the source will saturate the detector and the only effective solution is to employ optical attenuation. Any attenuation element shall not reduce the numerical aperture of the optical system and shall not be the source of significant reflections or optical distortions, which will bias the resulting encircled flux.

NOTE 1   When neutral density filters are used in the optical system, geometric distortions may can be introduced.

NOTE 2   Changing the attenuation between the optical centre image and the image of the measured source may can cause the location of the optical centre of the measurement source to move away from that determined using the optical centre image, causing errors in the resulting radial data functions.

6.1.7 Micro positioner (optional)

The micro positioner is an optional part of the apparatus. Depending on the apparatus design, it is possible to rely on connector ferrule geometry to place the image completely onto the detector without a micro positioner. In many implementations, only a focus adjustment (Z axis) is necessary, and in some cases, all three axes may only require alignment during construction or maintenance of the apparatus. Using the ferrule to place the fibre core image onto the detector does not relieve the requirement of finding the optical centre as required by 9.3.

When used, the purpose of the micro positioner is to bring the projected image of the fibre face into focus on the detector and to determine the magnification of the apparatus (see Clause 8). Mechanical locking mechanisms or their equivalents are required for all three axes to prevent mechanical drift during measurement. The micro positioner can optionally be driven by motors and can optionally employ feedback mechanisms to control the actual position of the stage (and thus the fibre face). ~~When geometric calibration is done using the micropositioner (see Clause 7 and Annex C), the performance requirements are specified in Annex B; otherwise, the only performance requirement is in the focal axis, which shall have high enough resolution to bring the fibre end into sufficient focus to achieve the required measurement precision.~~

6.1.8 Input port

The input port is where the calibration artefacts and measurement samples are connected to the apparatus. The input port characteristics depend on which type of source is to be characterized.

When characterizing transmission light sources, the input port is the distal end of the test jumper assembly. The proximal end of the test jumper assembly will be imaged onto the detector. When a micro positioner is used, the proximal end will be attached to the micro positioner.

When characterizing measurement light sources, the input port is commonly a connector bulkhead or its equivalent. When a micro positioner is employed, the bulkhead will be attached to the micro positioner.

See 6.2 and 6.3 for particular requirements.

6.1.9 Calibration light source

The calibration light source is used when calibrating the apparatus (see Clause 8). When this source is used to illuminate the test jumper assembly, the calibration source shall overfill the modes of the jumper. Optionally, a mode scrambler ~~may~~ can be used with the chosen calibration source to ensure more uniform overfilling of the fibre. See IEC 60793-1-41 for information on mode scramblers.

Any spectrally broad non-coherent light source, such as a tungsten-halogen lamp, a xenon arc lamp, or a light-emitting diode (LED), ~~may~~ can be used to overfill the fibre of the test jumper assembly. When calibrating the apparatus for the characterization of measurement light sources, the centre wavelength of the calibration source shall be within 30 nm of the nominal wavelength of the light sources to be qualified, and its spectral width (i.e., full width at half maximum) shall be no more than 100 nm. When calibrating the apparatus for the characterization of transmission light sources, the spectral characteristics of the calibration source are not specified, but it is recommended that its spectrum be similar to the sources to be characterized. The chosen calibration source shall be stable in intensity over a time period sufficient to perform the measurements.

6.2 Transmission source apparatus

6.2.1 General

When characterizing transmission light sources, the input port of the apparatus consists of two elements, the test jumper assembly and the fibre shaker (see Figure 2 below).
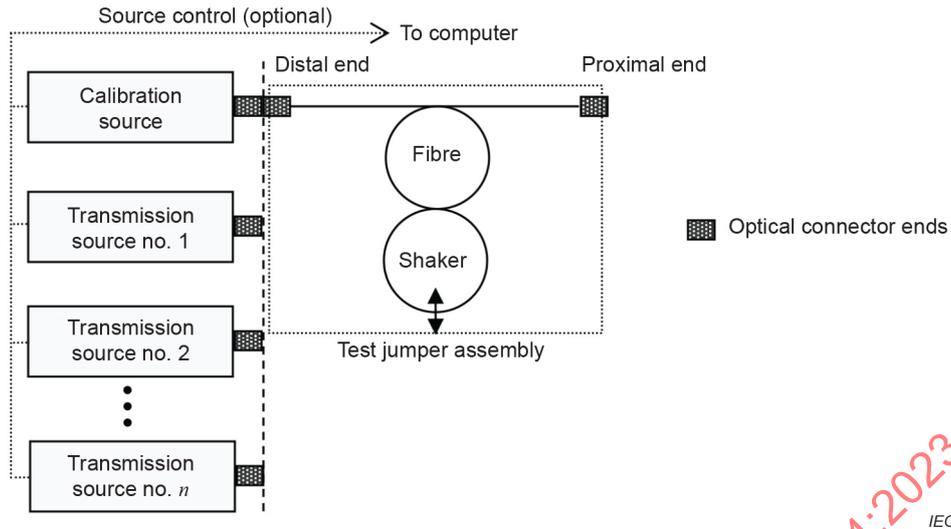
Figure 2 – Typical set-up for transmission source measurement

6.2.2 Test jumper assembly

The purpose of the test jumper assembly is to strip cladding modes, and to allow speckle to be averaged out by mechanical flexing of a portion of the test jumper assembly. The test jumper assembly is used only when qualifying light sources for multimode transmission.

The test jumper assembly shall be at least 10 m in length, made of germanium-doped near-parabolic graded-index fused-silica multimode "glass", an IEC 60793-2-10 class A1-OM2 to OM5 fibre with a core diameter of either 50 µm or class A1-OM1 fibre with a core diameter 62,5 µm. The test jumper assembly shall consist of a single, uncut length of fibre with connectors at each end. The test jumper assembly connectors shall have single-mode mechanical tolerances, even though the fibre is multimode.
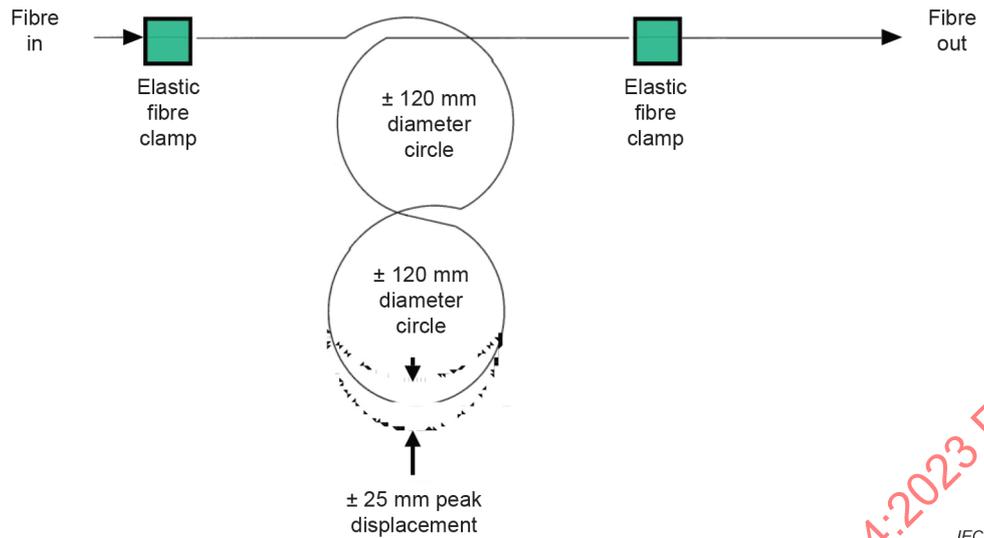
6.2.3 Fibre shaker

The purpose of the fibre shaker is to change the differential path length of the various modes in the test jumper, ensuring that speckle in the averaged image will be reduced, as the image is averaged. Speckle reduction can be accomplished in a variety of ways and shall be good enough to ensure sufficient repeatability in the measurement of encircled flux. Shaking of the test jumper assembly with a mechanical device is required to reduce speckle.

Part of the test jumper assembly shall be mechanically shaken continuously in each of three nominally orthogonal directions (using three independent shaker mechanisms) during the measurement, making at least one hundred shake cycles in each of the three directions during the measurement period. The shake frequencies in the three directions shall be chosen such that the three shake cycles synchronize no more often than once every five hundred cycles of the middle shake frequency.

A fibre shaker mechanism may can be of any design as long as it induces large amplitude movements and flexing in the optical fibre. Fibre transverse displacements of more than 25 mm are suggested. The fibre shakers shall include a fibre holding fixture for securely holding the fibre.

One exemplary mechanism, shown in Figure 3, has three turns of fibre coiled into a 3-ply figure-eight arrangement, with the loops each being approximately 120 mm in diameter. A motor-driven eccentric drives a slider back and forth at about one stroke per second, alternately flattening and stretching one loop of the figure eight with 25-mm amplitude. Three such mechanisms in series will consume about $3 \times 3 \times (2 \times \pi \times 0,120) = 6,8$ m of the test jumper assembly's fibre.

NOTE 1   Only one figure-eight loop of the three loops is shown here, for visual clarity. Fibre clips are used to keep fibre in place, in addition to elastic fibre clamps that prevent transmission of fibre motion. Loose fibre clips not shown.

NOTE 2   Fibre is moved back and forth as shown, with a peak-to-peak amplitude of about 25 mm, distorting one fibre loop.

Figure 3 – Fibre shaker example

Another exemplary approach is to hang large loose loops of fibre in front of a large fan which blows these loops about, the turbulence in the stream of the fan randomizing the motion.

NOTE 1   The fibre ends leading into and out of the fibre shakers are mechanically fixed or stabilized to prevent movement of fibres at connection points. In addition, the fibre shakers are mechanically isolated from the rest of the test setup so that vibrations are not transmitted to connection points throughout the apparatus, or to the micro positioner, detector, or magnifying optics. Vibration reduction is easier if the fibre shaker is both statically and dynamically balanced, and if all moving components are light in weight.

NOTE 2   There is no required relation between the measurement period (containing the one hundred strokes) and the acquisition time of an image. Typically, in each measurement period, many individual images are taken and later summed or averaged by the computer; this technique ~~may~~ can help to avoid detector saturation. The detector and digitizer ~~may be able to~~ can perform an equivalent function independently. The image will be relatively speckle free when one hundred shake cycles are averaged in this way.

6.3   Measurement source apparatus

The apparatus as described in 6.1 is sufficient to characterize measurement light sources. Fibre shaking or other speckle reduction techniques shall not be employed.

NOTE   This document does not address the characterization of OTDR transmitters, which will display significant speckle. At the time of publication of this document, the characterization of encircled flux for OTDRs was still under study.

7   Sampling and specimens

Light sources to be tested shall be chosen and prepared as defined by the user of this document, who shall document the sampling and preparation procedures used. The only requirements on the light sources under test are that they have an operating wavelength compatible with the detector and have optical connectors or splices compatible with the input port of the apparatus. The construction details of the light sources are otherwise unspecified.

When qualifying lasers, the laser drive current shall be sufficient to ensure that the laser always acts as a laser, rather than as a light-emitting diode (LED).

8   Geometric calibration

Calibration of the apparatus is critical to the accuracy of this measurement procedure (see Clause A.4 for a description of the kinds of noise and errors that calibration can correct). Calibration shall be performed periodically and should be performed at least monthly. If the calibration is known to drift significantly during a measurement interval, the source(s) of the drift shall be identified and eliminated. If the apparatus is disassembled, or its components in the optical path or affecting the optical path are otherwise manipulated, calibration shall be performed before measurements are made.

The purpose of geometric calibration is to obtain the measurement data needed to compute the magnification factors S_X and S_Y which have units of microns per pixel. These factors will be used to convert camera coordinates to fibre end-face coordinates. These magnification factors can be arrived at by either using IEC 61745 (specifically 2.3.4.1 "Scaling Factor") or by using the micropositioner as outlined in Annex B using IEC 61745:2017 (specifically 5.3.4.2). The micropositioner calibration method is an acceptable calibration method when the test apparatus is to be used to qualify transmission sources. The IEC 61745 method is the preferred calibration method for all types of light sources. The calibration for use with transmission type light sources may alternatively be done by means of the micropositioner method.

9   Measurement procedure

9.1   Safety

All procedures in which an LED or laser source is used as the optical source shall be carried out using safety precautions in accordance with IEC 60825-1.

9.2   Image acquisition

9.2.1   Raw image acquisition

9.2.1.1   General

Acquiring an image is central to the measurement of encircled flux. The approach to image acquisition depends on the general characteristics of the light source being measured. When acquiring transmission light source images, a fibre shaker is required, which in turn requires that some form of averaging be performed.

Measurements of light sources, on the other hand, will not require a fibre shaker, and usually their optical intensity is sufficient to allow very short detector integration times. These issues are discussed in 9.2.1.2 and 9.2.1.3.

In any case, the raw image obtained from the measurements described in 9.2.1.2 and 9.2.1.3 is a matrix of uncorrected intensities I_{raw}, whose dimensions are N_r rows by N_c columns.

9.2.1.2   Transmission light source image acquisition

Since transmission light sources require a fibre shaker, and the resultant image shall be integrated over at least 100 cycles of the fibre shaker, long integration times are required. Direct detector integration and digital image accumulation may can be employed to achieve the required integration. A typical procedure is to acquire multiple frames and sum or average them numerically, pixel-by-pixel. This approach prevents detector saturation while integrating enough shaker cycles to effectively reduce speckle.

9.2.1.3   Measurement light source image acquisition

Typical measurement light sources require only one short-period detector integration to arrive at a usable raw image. These sources are sufficiently incoherent and are sufficiently intense to

easily get adequate dynamic range, although attenuation may be required to operate the detector within its linear range.

NOTE   OTDR measurement light sources present significant challenges to applying this method and have not been investigated.

9.2.2   Dark image acquisition

The dark image is used to correct the raw image, pixel-by-pixel, for dark currents and DC offsets ~~from~~ introduced by the detector and digitizer. To acquire the dark image, the detector integration time and digital image accumulation shall be the same as was used to acquire I_{raw}. The dark image is acquired with the input port of the apparatus blocked to prevent light from entering the optical system. The resultant image is the matrix I_{dark}.

In some systems, ~~it may be shown that~~ the dark image is sufficiently uniform to be assumed ~~to be~~ constant for all pixels. In this case, each element of I_{dark} can be taken as zero. The average dark level will be removed from the resultant data by the baseline subtraction procedure outlined in 10.2.

9.2.3   Corrected image

The corrected image matrix I, is computed from the matrices I_{raw}, I_{dark} and ~~U~~ $U_{r,c}$ as shown in Formula (1).

$$I_{r,c} = \left(I_{raw_{r,c}} - I_{dark_{r,c}} \right) * U_{r,c} \tag{1}$$

where

$U_{r,c}$ is the sensitivity correction matrix, reducing non-uniformity of the detector's pixel-to-pixel conversion efficiency.

NOTE 1   The asterisk (*) operator denotes element-by-element multiplication.

NOTE 2   When the camera is sufficiently uniform without correction, and the baseline subtraction step of 10.2 is to be performed, no correction is required, so I can be set to I_{raw}.

9.3   Optical centre determination

9.3.1   General

Encircled flux is computed with respect to the optical centre of the multimode fibre's core. It is known that coherent light sources can produce, at least over short distances, near fields which are not symmetric about the centre of the fibre core. When measuring transmission sources, which are typically coherent, the optical centre of the test jumper assembly cannot be determined from the nearfield image of the transmission light source itself. Instead, the test jumper assembly's centre is determined by illuminating its core with a calibration source and finding the centroid of the resulting nearfield.

~~NOTE~~   Since transmission light sources require two separate images to make a measurement of encircled flux (i.e., the image for centring and an image of the light source to be measured), attenuation setting is more challenging. As previously noted, moving or changing the attenuation between two images can shift the optical centre of the image. It is recommended that one attenuator setting be used for both images.

9.3.2   Centroid image

The centroid image is the image used to determine the optical centre of the multimode fibre cord. As discussed above, the centroid image for transmission light sources is an image of the

test jumper assembly illuminated by a calibration light source. For measurement light sources, the same image shall be used to find both the optical centre of the fibre and to compute the encircled flux. Use 9.1 to acquire the centroid image.

NOTE   A transmission light source centroid image can be used for any number of measurements of encircled flux as long as the test jumper assembly's optical centre is sufficiently stable with respect to the detector. Stability of the micro positioner, if used, and reasonable control of the ambient environment help ensure that the test jumper remains fixed in place.

9.3.3   Centroid computation

Using the centroid image, the near field centre is computed by finding the centre of gravity of the light intensity distribution for each Cartesian axis independently.

To find the centroid, first find P_{Max} and P_{Min} respectively, which are the intensities of the brightest and dimmest valid pixels in the entire centroid image (using invalid pixels will corrupt the determination of T), and then compute the threshold T as shown in Formula (2).

$$T = 0{,}1 \left(P_{Max} - P_{Min} \right) + P_{Min} \tag{2}$$

Next, compute the three summations shown in Formula (3) over all pixels, excluding pixels with intensities less than T, over the row and column indices r and c.

$$
\begin{aligned}
S_P &= \sum_{r=1}^{N_R} \sum_{c=1}^{N_C} \begin{cases} 0 & I(r,c) < T \\ I(r,c) & I(r,c) \geq T \end{cases} \\
S_r &= \sum_{r=1}^{N_R} \sum_{c=1}^{N_C} \begin{cases} 0 & I(r,c) < T \\ r\,I(r,c) & I(r,c) \geq T \end{cases} \\
S_c &= \sum_{r=1}^{N_R} \sum_{c=1}^{N_C} \begin{cases} 0 & I(r,c) < T \\ c\,I(r,c) & I(r,c) \geq T \end{cases}
\end{aligned}
\tag{3}
$$

Finally, compute the coordinates of the centroid, (X_0, Y_0), as shown in Formula (4).

$$
\begin{aligned}
X_0 &= \frac{S_c}{S_P} \\
Y_0 &= \frac{S_r}{S_P}
\end{aligned}
\tag{4}
$$

9.4   Test source image acquisition

To acquire an image of the test source, connect the test source to the apparatus and energize the test source. Allow the test source to warm up as required, and then acquire an image of the test source using the guidelines in 9.1.

10 Computation of encircled flux

10.1 Computation of radial data functions

The first computation step reduces the 2D pixel data into a one-dimensional (1D) radial function by averaging the pixels in sets of nested and overlapping annular rings of thickness $2W$ (where W is 0,2 µm unless otherwise specified), which are centred on the optical centre of the fibre, X_0, Y_0, as defined in 9.3.3. The spacing of the rings is W microns, although the ring's radial coordinate in the resulting radial data functions will be the radial centroid of the radial coordinates of the pixels in the ring.

The filtering concept is illustrated in Figure 4. The elements of the square grid are the pixels of the image. Two rings, centred on the optical centre X_0, Y_0, are shown: the outer ring is hatched vertically, and the inner ring is hatched horizontally. Each ring has a width $2W$ and overlap in a region W wide. The overlap region in the diagram is cross-hatched. The greyed-in pixels are the pixels which will be averaged into the outer ring since their centres fall inside the outer ring's boundary.

Figure 4 – Pixel and ring illustration

Use the following steps to compute the radial functions.

a) Determine the maximum radius of a complete ring. This step finds the largest ring that will fit in the image without being truncated by an image boundary. Compute the shortest distance to the edge of the image from the image centre using Formula (5).

$$
\begin{aligned}
D_{\mathsf{L}} &= S_{\mathsf{X}} X_0 \\
D_{\mathsf{R}} &= S_{\mathsf{X}} \left(N_{\mathsf{C}} - X_0 \right) \\
D_{\mathsf{T}} &= S_{\mathsf{Y}} Y_0 \\
D_{\mathsf{B}} &= S_{\mathsf{Y}} \left(N_{\mathsf{R}} - Y_0 \right) \\
D &= \min \left(D_{\mathsf{L}}, D_{\mathsf{R}}, D_{\mathsf{T}}, D_{\mathsf{B}} \right)
\end{aligned}
\tag{5}
$$

Where the function "min" finds the minimum of the four distances. Next, compute the number of rings, N_R, as shown in Formula (6).

$$N_R = \frac{D - W}{W} \qquad (6)$$

a) Allocate and zero the three summation arrays, $S_R(0..N_R)$, $S_I(0..N_R)$, and $S_N(0..N_R)$.

For each and every pixel (on row r and column c), perform the following steps.

b) Compute the radial coordinate R as shown in Formula (7).

$$R = \sqrt{S_Y^2 (r - Y_0)^2 + S_X^2 (c - X_0)^2} \qquad (7)$$

c) Compute the ring index i as shown in Formula (8).

$$i = \text{trunc}\left(\frac{R}{W}\right) + 1 \qquad (8)$$

d) If i is less than or equal to N_R, then sum into both ring i and ring $i - 1$, as shown in Formulae (9) and (10).

$$
\begin{aligned}
S_R(i) &= S_R(i) + R \\
S_I(i) &= S_I(i) + I(r,c) \\
S_N(i) &= S_N(i) + 1
\end{aligned}
\qquad (9)
$$

$$
\begin{aligned}
S_R(i-1) &= S_R(i-1) + R \\
S_I(i-1) &= S_I(i-1) + I(r,c) \\
S_N(i-1) &= S_N(i-1) + 1
\end{aligned}
\qquad (10)
$$

The above double sum implements the overlapping-ring smoother.

e) Finally, compute the parametric function pair (where i is the parameter) for each ring by computing the average radius $\overline{R}$ and average intensity $\overline{I}'$ in each ring as shown in Formula (11).

$$
\begin{aligned}
\overline{R}(i) &= \frac{S_R(i)}{S_N(i)} \\[2mm]
\overline{I}'(i) &= \frac{S_I(i)}{S_N(i)}
\end{aligned}
\qquad (11)
$$

NOTE Depending on the camera's resolution and the ring thickness selected, it is possible for some of the interior rings to contain no pixels, so the corresponding S_N values will be zero. In this case, the ring should be omitted, the subsequent array elements should be shifted up, and N_R should be decremented. It is also possible for two or more adjacent rings to have the same $\overline{R}$ (or trivially identical, say within 0,01 µm). In these cases, the radii and intensities in these adjacent rings should be averaged, and those rings replaced with one ring of averaged $\overline{R}$ and averaged intensity, and N_R should be decremented appropriately.

10.2 Integration limit and baseline determination

10.2.1 Integration limit

The general equation for encircled flux is given by Formula (12).

$$EF(r) = \frac{\displaystyle\int_0^r r'I(r')dr'}{\displaystyle\int_0^\infty r'I(r')dr'} \tag{12}$$

The measurable nearfield intensity does not extend very far beyond the fibre's core boundary, and so it is justifiable to truncate the denominator integral at a radius somewhere beyond the core. From a measurement perspective, extending the integral far beyond the core only integrates noise and so only increases the noise of the measurement.

The integration limit, R_{Max}, shall be set to 1,15 times the nominal core radius of the fibre connected to the test source. For example, R_{Max} would be set to 28,75 for 50 µm fibres. The maximum index, i_{Max}, can then be found as the index of the first radius in $\overline{R}(i)$ that is greater than or equal to R_{Max}.

10.2.2 Baseline determination

Determine the average baseline intensity, B, as the average of a set of $\overline{I}'(i)$ nearby, but outside the core's nearfield. The set of points shall include points from R_{Max} outwards in radius. The limit where averaging shall be terminated, unless otherwise specified, shall be at radii no greater than 1,2 times the nominal core radius of the fibre connected to the light source.

10.2.3 Baseline subtraction

Compute the baseline-subtracted intensity function, $\overline{I}(i)$, as shown in Formula (13).

$$\overline{I}(i) = \overline{I}'(i) - B \qquad 0 \le i \le i_{\text{Max}} \tag{13}$$

10.3 Computation of encircled flux

The computation of encircled flux is done in two steps: first, integrating the radius-weighted radial data function, $\overline{R,RI}$ $\overline{R}(i) \times \overline{I}(i)$, and then normalizing the function to a maximum of unity. This process will produce another parametric function pair, $\overline{R}$ and EF.

To compute the integral, it has been shown that simple summation or rectangular rule integration produce errors of approximately 0,25 %. These errors can easily be avoided by employing higher-order integration methods. Trapezoidal rule integration is shown in Formula (14) (the special case at index zero stems from the fact that the radius-intensity product at zero radius is identical to zero).

$$EF'(i) = \begin{cases} \dfrac{\overline{R}(0)^2 \overline{I}(0)}{2} & i = 0 \\ EF'(i-1) + \dfrac{\overline{R}(i)\overline{I}(i) + \overline{R}(i-1)\overline{I}(i-1)}{2} \times \left[\overline{R}(i) - \overline{R}(i-1)\right] & 0 < i \leq i_{\text{Max}} \end{cases}$$

(14)

The function $EF(i)$ is then computed by normalizing $EF'(i)$ as shown in Formula (15).

$$EF(i) = \frac{EF'(i)}{EF'(i_{\text{Max}})}$$

(15)

In many cases, values of encircled flux at radial values other than the discrete values of $\overline{R}$ are required. It is sufficiently accurate to employ linear interpolation to produce these intermediate values.

11 Results

11.1 Information available with each measurement

Report the following with each measurement:

– date and time of measurement;
– identification of source specimen;
– nominal wavelength of source;
– radius and encircled flux at each radius specified in the detail specification, or if not specified, the radii and encircled flux data computed in Clause 10;
– EF as a graph as a function of radius, including any specified template limits.

11.2 Information available upon request

The following information shall be available upon request:

– date of most recent calibration of equipment;
– method of calibration of equipment;
– ring width, W, used in the computations;
– integration limit parameters, R_{Max} and i_{Max};
– original images used in the computations;
– geometric calibration factors, S_{X} and S_{Y};
– derived centre, and if different, the centroid image;
– radial data functions computed in 10.1.

12 Specification information

The detail specification shall specify the following information:

– type of source to be measured;

- sampling requirements, if any;
- criteria to be met by sources;
- any deviations to the procedure that may apply;
- radii at which the EF is to be reported;
- the EF template used to report results.
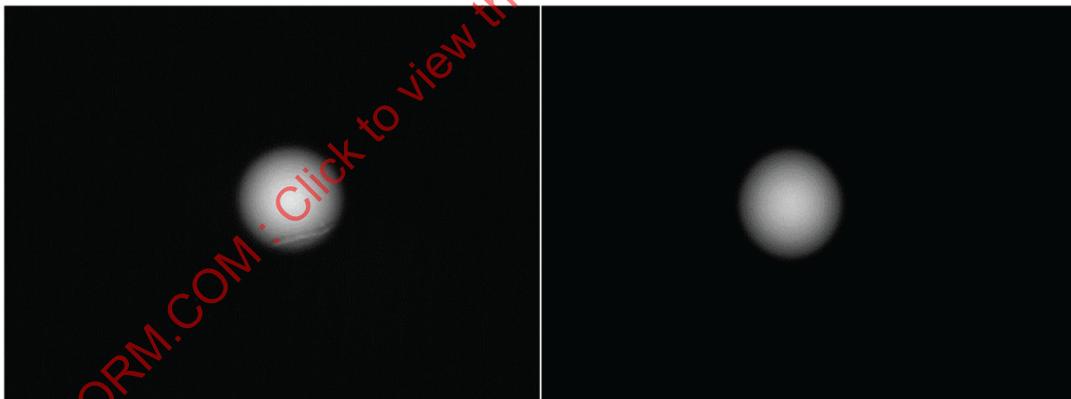
Annex A
(informative)

Measurement sensitivity considerations

A.1   Baseline averaging considerations

A trade-off exists when selecting the region where baseline averaging is performed (see 10.3). The baseline value, B, is subtracted from the entire set of intensities. If the value of B is taken on a single intensity point, then the noise of the system would increase substantially (approximately by the square root of two).

Averaging a region of intensities decreases this noise contribution, if all points in the intensity function have uncorrelated noise, then the noise will increase by the square root of one plus the number of intensities averaged. However, imperfections in the optical system of the apparatus, or imperfections in the camera, can make the baseline region outside the core to be non-constant, and so averaging the entire baseline region may can cause a bias in B. Selecting an appropriate region over which to make the baseline determination should be done by characterizing the actual apparatus. Clause A.1 provides an analysis of two different images from two different instruments to illustrate methods an instrument designer might use to determine how far baseline averaging should extend into the intensity function.

The two images shown in Figure A.1 below are from two similar instruments (the instruments do not use like components). Both use analogue cameras and PC-integrated frame grabbers, and have similar effective pixel sizes. The images show two different, but similarly filled, 50 µm fibre cores. Instrument A shows a small imperfection on the lower portion of the core, but for this analysis, this imperfection is not important.

Figure A.1 – Core images from instrument A and instrument B

It is useful to modify the display of the images such that pixels lower than the average background intensity are set to black, and pixels above the average background intensity are set to white to see, which reveals small non-idealities ideal features in the images. Figure A.2 below shows the two images from Figure A.1 reprocessed in this way.
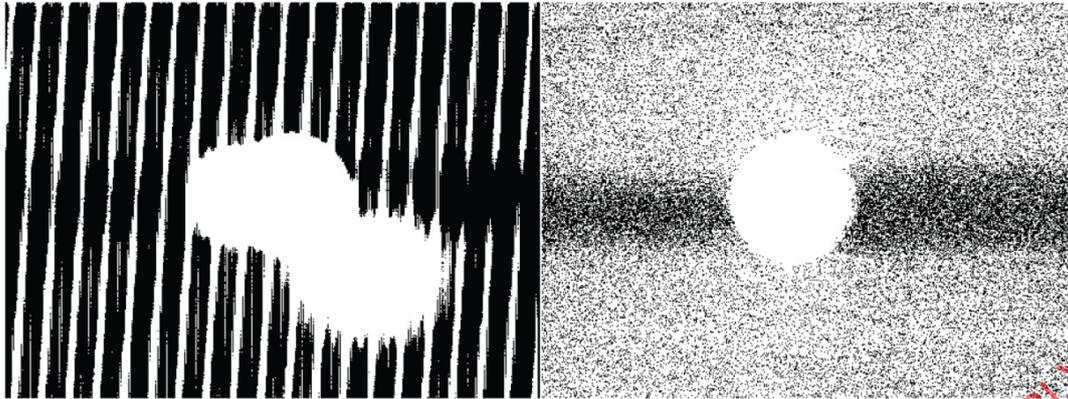
Figure A.2 – Compressed core images from instrument A and instrument B

Instrument A shows a small amount of video pattern noise (the nearly vertical white and dark pattern). Instrument A also shows two white spots not attributable to the core image (to the left and bottom-right of the image). These spots are most probably caused by small reflections in the optical system. Instrument B shows a small, horizontal stripe across the centre of the image. This section of the background has slightly less intensity than other regions of background in the image, which is caused by recovery artefacts in the CCD sensor used in the camera. When these images are processed to produce 1D radial functions as described in 10.1 and the resultant nearfield functions in the baseline are carefully examined, two different patterns emerge.

Since instrument A has a baseline which includes small reflections, the baseline is not constant. The flat section within the reflection region is also between the default averaging radii of 1,15 to 1,2 times the nominal core radius, as shown by the vertical dotted lines (see Figure A.3 below). The baseline near the core includes the additive effect of the reflections; these reflections extend into the image of the core, and so the best estimate of the baseline should include these reflections. If averaging occurred beyond the default averaging radii, the baseline would be biased downward.
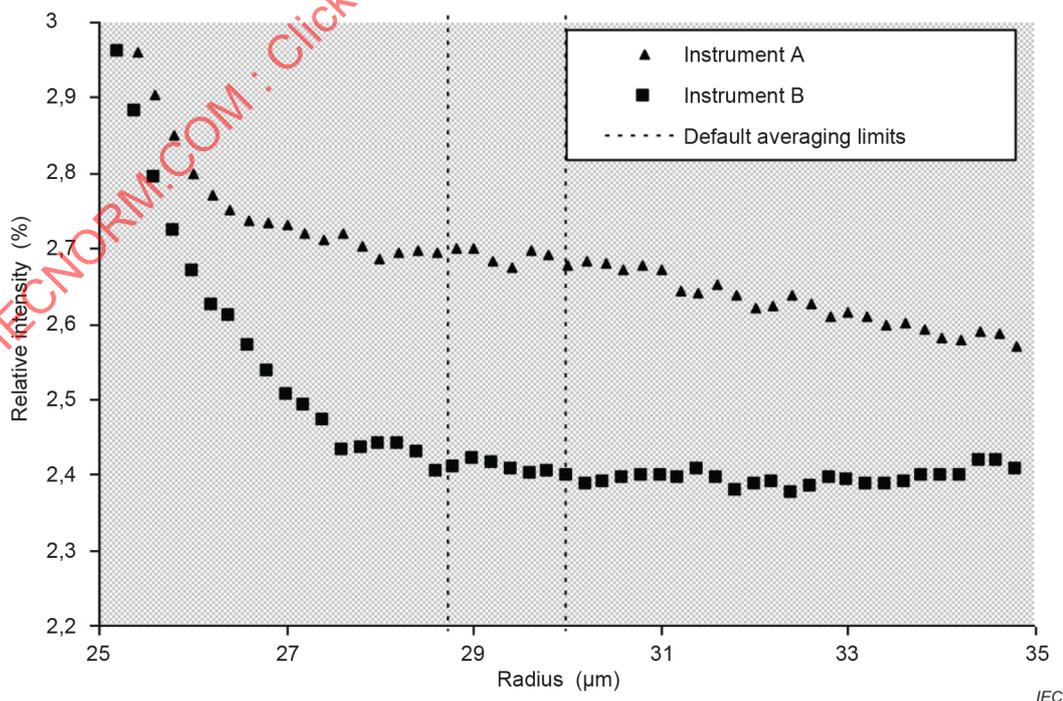

Figure A.3 – Intensity versus radius for instruments A and B

Instrument B has very small modulations in the baseline, and the baseline can be determined by averaging the entire set of data beyond the integration limit of 1,15 times the nominal core radius, thus reducing noise in its estimate.

A.2 Pixel sensitivity variation calibration

Perform the following procedure to determine the pixel sensitivity variation correction matrix $U_{r,c}$. Record the image, I_{uRaw}, on the detector when it is uniformly illuminated ~~with a uniform~~ (to within 1 %) ~~illuminated area bright enough to almost saturate~~ with the ~~camera~~ signal reaching about 75 % of the saturation level (the inside of a small integrating sphere works well as a uniformly illuminated area). Next, record the dark image, I_{uDark}, when the uniform source is off. Compute the average pixel, P_{uAvg}, as shown in Formula (A.1).

$$P_{uAvg} = \frac{\sum_{r=1}^{N_r} \sum_{c=1}^{N_c} \left(I_{uRaw_{r,c}} - I_{uDark_{r,c}} \right)}{N_r N_c} \tag{A.1}$$

Compute each element in ~~U~~ $U_{r,c}$ as shown in Formula (A.2).

$$U_{r,c} = \frac{P_{uAvg}}{I_{uRaw_{r,c}} - I_{uDark_{r,c}}} \tag{A.2}$$

The resulting element values will typically range from 0,90 to 1,10. They are to be multiplied by their corresponding pixels, so as to normalize those pixels to the average sensitivity of all pixels, for every measurement that is made.

A.3 Correlated double sampling

One can use "correlated double sampling" (CDS) to almost completely eliminate CCD camera offsets, and their temperature sensitivity, at the cost of some added equipment complexity. Correlated double sampling is also quite effective against uncorrelated stray light. Makers of specialized instruments intended to perform the measurements described in this document would be well advised to implement correlated double sampling.

To implement CDS, one blinks the laser or incoherent calibration source at a frequency somewhere between 5 Hz and 60 Hz, and electrically synchronizes the camera to the periodic blinking in such a way that odd frames are dark (source off), while the even frames see the nearfield to be measured (source on). The odd frames are subsequently subtracted from the preceding even frames, pixel for pixel, yielding an offset-corrected 2D nearfield flux distribution. For best calibration, the "on" time should exactly equal the "off" time. If ~~one is averaging~~ a series of frames is to be averaged, ~~add~~ then all even frames, ~~subtract~~ should be added, all odd frames should be subtracted from the sum of even frames, and ~~divide~~ the resulting difference should be divided by the number of even frames. CDS would replace the entire offset correction scheme in 9.2.3, but pixel sensitivity correction will still be required. If many measurements are to be made, like in a factory, this approach can be a time saver, as many sources of inaccuracy that would otherwise require time and care to ~~prevent~~ correct manually are simply eliminated. The ~~chosen~~ blink rate should be chosen to be an exact sub-multiple of the local power-line frequency, 50 Hz or 60 Hz, to ensure maximum discrimination against artificial stray light and electrical noise, so that an integral number of power frequency sine waves will fit in the time that the source is either on or off. For example, with 60-Hz power, the "on" time and "off" time

could both be 1/30 of a second (two complete cycles fit in the on period, and another two complete cycles fit in the off period), ~~for~~ yielding a blink rate of 15 Hz. It is not necessary to phase lock the sampling period to the power-line cycle period; it is sufficient that the sampling period be an exact multiple of the power-line cycle period.

A.4   Imperfections of practical detectors and optics

Cameras vary in their mechanical construction, age, condition, and state of adjustment. Some will contain two-dimensional detectors, where the distortions will be due largely to optics and non-square pixels. Some will mechanically scan a one-dimensional (linesman) CCD more or less perpendicular to its line of pixels. Some will mechanically scan a single pixel (a pinhole) in two dimensions. Others will scan a set of perhaps orthogonal slits over a single large-area detector. Imperfections in these mechanical scanners will cause the X-direction and Y-direction magnification to differ significantly, and non-perpendicular~~ity~~ movement of the various mechanical components can also cause shearing (where motion along one axis causes apparent motion in another axis). The camera body (or the CCD chip within) ~~may~~ can be slightly rotated about the camera's Z (optical) axis, and the camera ~~may~~ can also be slightly tilted with respect to the test jumper assembly's optical axis.

In mathematical terms, all of these geometric distortions can together be expressed as a single overall "affine transformation" between "true space" (micro positioner coordinates) at the fibre face and the "TV space" reported by the camera. Affine transforms are easily expressed with matrices. In practice, one measures the camera's distortions, derives the affine transform, and uses the transform to mathematically compensate subsequent measurements for the camera's geometric distortions. No two cameras will be exactly alike, so this compensation shall be done on a per camera basis (i.e., by serial number). In general, if a camera is working well, it is better to calibrate and compensate mathematically than to try to physically adjust the camera. However, in any case, one shall recalibrate whenever the camera is repaired or adjusted, or the mounting of components to the optical bench or optical plate is disturbed.

Dark current~~: dark current~~, which is caused by various kinds of electrical leakage within the photodiodes of the CCD chip at the heart of the camera, is a very sensitive ~~to~~ function of temperature, typically doubling for each seven degrees centigrade rise in chip temperature. No two pixels (or CCDs) will have exactly the same dark current. Because dark current is integrated during each exposure period, the output voltage offset induced by dark current will vary in direct proportion to exposure duration (integration time).

~~Fixed-pattern noise:~~ Fixed-pattern noise, which is due to capacitive feedthrough of logic clock signals into video lines within the CCD chip, has a repetitive and usually complex pattern that does not vary significantly with temperature, illumination, or exposure duration. The pattern is fixed from pixel to pixel; any given pixel will have a substantially constant value.

Pixel crosstalk noise~~: pixel crosstalk~~, which is caused by imperfect charge transfer from pixel to pixel as the image is being shifted to the output, causes smearing of the image and bleeding into background areas.

Under reasonable laboratory conditions, the offsets introduced by dark current and fixed-pattern noise combined with pixel crosstalk ~~combined~~ are typically no more than about 5 % or 10 % of saturation, if stray light has been fully eliminated and the exposure duration is short enough for the temperature.

Pixel sensitivity variation is an effect where the sensitivity (responsivity) of individual pixels to light varies by up to ±10 % from the mean due to manufacturing variations, but does not vary significantly with temperature, illumination, or exposure duration, so long as both saturation ceiling and noise floor are avoided.

Bad pixels~~: a few~~ are pixels that have little sensitivity to light, remaining stuck at some high or low value, or being very much less sensitive to light than average. Because even 100 bad pixels

out of the 30 000 active pixels in a 256 x 256 picture have negligible effect on the results, one can simply ignore bad pixels in the procedures described in this document, except when determining the centroid threshold, making no attempt to eliminate or compensate for bad pixels.

The above paragraphs discussed the imperfections of the imager chip itself. However, the optical system containing the imager has imperfections as well, in addition to the mechanical misalignments that are calibrated out in Clause 8 and Annex C. For the purposes of this document, the principal imperfections are caused by internal reflections in the optical system, especially reflections within and between the microscope objective and the detector. Reflections can be produced at any optical discontinuity, but especially at air/glass interfaces. These interfaces can be found at the outer surfaces of the magnifying optics, attenuators and filters, beam splitters and the window of the detector package that protects the imager chip. It is possible to use windowless detector packages; this practice may can expose the imager chip to the environment causing reliability problems. The degree to which these reflections affect the measurement of encircled flux depends on the location of the reflections within the image, the reflection's intensity, and the shape of the reflection.

The useful way to tell if a spot in an image is caused by a reflection is to move the fibre end-face (input port) in the XY plane, and observe the resulting motion of the spots. Reflections will generally move along the line of fibre end-face motion, but at a greater or lesser speed than the direct image of the fibre end-face, and often in the opposite direction. Compressing and false-colouring these images, as demonstrated in Figure A.2 may can help in detecting these reflections.

The most common remedy is the use of anti-reflection coatings on all optical surfaces, and this works reasonably well if the test wavelength is well matched to the wavelength range for which the coating was designed.

In addition, one can arrange the optical system such that reflections fall into harmless locations. The simplest way to accomplish this is to move the centre of the fibre face to one side of the microscope objective's optical axis and the centre of the imager chip to the other side, while maintaining the various planes (image, object, and principal) in parallel, depending on the flat field of the objective to maintain focus despite these displacements. Then, light from the objective will arrive at an angle to the window, and will be reflected off to one side.

The parallel-displacement approach mentioned above is a special case of the "Scheimpflug condition", which is the principle behind view cameras in photography. The Scheimpflug condition is met when the image plane, the object plane, and the corresponding lens principal planes all intersect the same line. This intersection line will be well away from the image or object, and in the case of parallel displacement, will be at infinity.

When the Scheimpflug condition is met, the image will be in perfect focus despite the tilted image, lens, and object planes. With parallel planes, the magnification factors do not depend on location in the image; while with intersecting planes, the magnification factors will vary linearly with location in the image. This varying magnification factor is easily handled using projective geometry, but the considerable added complexity did not seem justified, as the parallel planes and affine geometry of this document approach are adequate.

Annex B
(informative)

Theory of geometric calibration using the micropositioner

B.1   Background and assumptions

The purpose of the procedure developed and documented here is the calibration of optical systems using mechanical positioning stages for use in this standard.

There are two coordinate systems of interest here, that of the mechanical positioning stage (called variously the object or the true coordinate system) and that of the camera (called variously the video or image coordinate system). The optical fibre whose nearfield is being measured physically exists in the object space, and is projected by a microscope objective onto the sensitive area of the imaging chip (within the camera) to form the image.

The XY planes of the two coordinate systems are parallel to one another, and are perpendicular to the optical (Z) axis of the microscope objective.

The X and Y (row and column, respectively) axes of the camera are assumed to be exactly perpendicular to one another, both by convention and because in practice the rows and columns of imager chips have essentially perfect orthogonality.

The X and Y axes of the mechanical stage are assumed to be nearly but not exactly perpendicular to each other, the skew angle (deviation from orthogonality) not exceeding $\pm 5°$.

The rotation of the image coordinate system with respect to the object coordinate system is assumed to not exceed $\pm 5°$.

These $\pm 5°$ limits are based on the expected maxima in practical systems, and the procedure developed here will actually handle angles up to a bit less than $\pm 45°$. The worst case is at the limit, with skew and rotation angles having opposite signs.

Whatever the values of the rotation and skew angles, they are expected to be constant once the components of the optical system are bolted together and locked.

Without loss of generality, the rotation angle is measured between the two X axes, and so the angle between the Y axes will be the algebraic sum of rotation and skew. In other words, all of the skew is by convention allocated to the Y axis of the object coordinate system.

The origin of the object (mechanical stage) coordinate system is likely to be remote from the outline of the fibre core and also from the origin of the image (camera) coordinate system, as mechanical stages usually have travel ranges in the millimetres. The origins are usually at a corner, and are rarely in the centre of either object or image plane.

To summarize, the coordinate system of the camera imager will in general be slightly rotated with respect to that of the stage, the axes of the stage will not be quite perpendicular, the origins of the two systems will not in general coincide, and the optical axis of the objective lens will usually fall well away from either origin.

The magnifications (scaling factors S_X and S_Y) in the X and Y (column and row) directions are not in general equal, although their ratio usually falls between 1:2 and 2:1, with 1:1 signifying square pixels. Scaling arises from two distinct physical causes. The first is the general ~40x magnification due to the microscope objective, which magnification will in general be exactly the same in all directions in the image planes. The second is due to the shape of the pixels in

the camera, and this will in general be different in the row and column directions of the imager chip, as the pixels are rectangular and not necessarily square. In practice, these effects are merged into a pair of overall scaling factors which in effect give the X and Y dimensions of an imager pixel as projected upon the face of the fibre in object space, with the effects of rotation and skew mathematically removed. This rotation will appear to be a rigid-body rotation only if the imager pixels are exactly square. Because the fibre has no preferred or distinguished orientation, for simplicity the axes of the imager are used.

One objective is commonality with IEC 61745, in particular by use of the same definition of S_X and S_Y as provided in 2.3.4.1 of that standard, such that one can use S_X and S_Y values generated using the IEC 61745, 2.3.4 approach for S_X and S_Y in this standard. Both S_X and S_Y are the ratio of object-space (IEC 61745: calibrated) motion to corresponding image-space (IEC 61745: measured) motion, aligned along the CCD row and column axes respectively. The units of S_X and S_Y are microns per pixel.

B.2 Mathematical development

After mechanically assembling the optical system consisting of stage, fibre, microscope objective lens, and camera, calibration is required. This is accomplished by illuminating the fibre with light of reasonable spectral width and reasonably symmetric nearfield intensity distribution, and moving the fibre in the object XY plane to three well-separated non-collinear positions. At each position, the X and Y coordinate settings of the stage are recorded and an image is captured. In each image, the centroid of flux exceeding a threshold is computed (as described in 8.3.3) and used as the corresponding position in image space.

NOTE 1 If different light sources are used for calibration and for subsequent nearfield intensity distribution measurement, the spectra of the two sources should be similar in center wavelength and perhaps spectral width, as the magnification factor of microscope objectives varies with wavelength.

For accuracy, each of the calibration positions shall be far enough from all edges of the image frame that no above-threshold pixels are clipped by an encroaching frame edge. Also, the response of the imager chip to illumination shall be substantially linear, so saturation shall be avoided. The best arrangement of points is a big, roughly equilateral triangle, or a right triangle. The exact shape isn't critical, so long as it roughly follows the edges of the frame, sufficiently far from the edges to avoid clipping off parts of the calibration-point nearfields.

One can test for adequate non-collinearity and adequate separation of the calibration points by computing the area of the triangle formed by the calibration points, and requiring that the ratio of triangle area to image-frame area exceed some minimum value. This may be done in pure pixel coordinates, without regard for the actual shape of the pixels, as pixel shape will cancel out in the ratio of areas.

All information needed to compute the X-axis and Y-axis scaling factors despite rotation, skew, and translation is contained in the locations of the three calibration points as seen in object and image space.

The first step is to compute the homogeneous affine transform matrix describing the relationship between object and image planes.

The general form of the transform is :

$$p'_i = M \times p_i \qquad (B.1)$$

where

$$p_i = \begin{bmatrix} x_i \\ y_i \\ 1 \end{bmatrix} \text{ and } p'_i = \begin{bmatrix} x'_i \\ y'_i \\ 1 \end{bmatrix}$$

are the locations of the ith calibration point in *object* and *image* space respectively,

$$M = \begin{bmatrix} a & b & c \\ d & e & f \\ 0 & 0 & 1 \end{bmatrix}$$ is the affine transform matrix in homogeneous form,

, and the × symbol means matrix multiplication.

Considering the transform matrix M, the physical interpretation of the elements $a \cdots f$ follow: a is the nominal magnification in the X direction (but is not S_x); b is the apparent motion in X due to real motion in Y; c is the translation in X; d is the apparent motion in Y due to real motion in X; e is the nominal magnification in the Y direction (but is not S_y); and f is the translation in the Y direction.

To compute M from the calibration points requires some matrix math. The derivation follows.

The first step is to form a linear system consisting of the three points and the matrix to be found:

$$P' = M \cdot P \tag{B.2}$$

where $P' = \begin{bmatrix} p'_1 & p'_2 & p'_3 \end{bmatrix}$ and $P = \begin{bmatrix} p_1 & p_2 & p_3 \end{bmatrix}$ are row vectors whose elements are column vectors, with primed symbols describing points in image space while unprimed symbols describe points in object space.

The next step is to solve for M:

$$M \cdot \left(P \cdot P^{-1} \right) = P' \cdot P^{-1} \tag{B.3}$$

$$M = P' \cdot P^{-1} \tag{B.4}$$

where P^{-1} signifies the matrix inverse of P.

Note that the homogeneous space is closed under matrix multiplication. So, all operations that yield a position vector should automatically yield "1" (within roundoff error) as the last element, and all operations that yield a transform matrix should automatically yield {0,0,1} (also within roundoff error) as the last row. If these constants fail to automatically emerge from the computations, there is an error in the code. It is useful to test that such assertions are always met, as their failure indicates that the results of further computations will at least be in error, and may be total nonsense.

NOTE 2 Although not required in the present algorithm, after testing for ≈0 and ≈1, it is common to round these constants to exactly zero or exactly one as appropriate, to reduce the accumulation of small numerical errors.

The upper left 2x2 sub-matrix (consisting of all but the constant and translation terms) of the transform matrix M contains all the skew, rotation and scaling information, uncontaminated by translations. As translations are no longer needed, the homogeneous form is also no longer needed, and the row containing the constants {0,0,1} may also be omitted, so what remains is the 2x2 sub-matrix containing only the elements a, b, d and e:

$$D = \begin{bmatrix} a & b \\ d & e \end{bmatrix} \tag{B.5}$$

The geometric transforms necessary to get from image space to object space are applied in a specific order, following in reverse the path of light from fibre face through lens to imager chip. Specifically, pixel scaling is first, implicitly followed by translation (to account for non-coincidence of the origins), followed by rotation of coordinate systems, and finally followed by skewing of the object coordinate system. The effect of translation will drop out regardless of where it is done in the light-path sequence, but order matters for all else.

First, the skew matrix:

$$K = \begin{bmatrix} 1 & \sin \varphi \\ 0 & \cos \varphi \end{bmatrix} \tag{B.6}$$

where φ is the skew angle, being the deviation from perpendicular (obliqueness) of the object coordinate system's X and Y axes.

Then, the rotation matrix:

$$R = \begin{bmatrix} \cos \theta & -\sin \theta \\ \sin \theta & \cos \theta \end{bmatrix} \tag{B.7}$$

where θ is the rotation angle, being the angle between the object and image X axes.

And finally the scaling matrix:

$$S = \begin{bmatrix} M_{\mathrm{x}} & 0 \\ 0 & M_{\mathrm{y}} \end{bmatrix} \tag{B.8}$$

where M_{x} and M_{y} are the inverses of the long-sought pure scaling factors.

To find the net effect, these matrices are multiplied in reverse order from that in which their effects are applied in the optical system. Their reverse order is a consequence of the formulation of Equation B.1.

$$D = S \times R \times K = \begin{bmatrix} M_{\mathrm{x}}\cos\theta & M_{\mathrm{x}}(\cos\theta\sin\varphi - \sin\theta\cos\varphi) \\ M_{\mathrm{y}}\sin\theta & M_{\mathrm{y}}(\cos\theta\cos\varphi + \sin\theta\sin\varphi) \end{bmatrix} \tag{B.9}$$

where θ is the rotation angle, φ is the skew angle, and M_{x} and M_{y} are the multiplicative inverses of the pure scaling factors (and are not equal to elements a and e unless the rotation and skew angles are both zero).

After application of some trigonometric identities, we have

$$D = S \times R \times K = \begin{bmatrix} M_{\mathrm{x}}\cos\theta & M_{\mathrm{x}}\sin(\theta - \varphi) \\ M_{\mathrm{y}}\sin\theta & M_{\mathrm{y}}\cos(\theta - \varphi) \end{bmatrix} \tag{B.10}$$

The objective is to isolate the inverse pure scaling factors M_{x} and M_{y} given only the numerical values for a, b, d and e derived from measurements at the calibration points.

The key observation is that if one tries to find these angles and inverse scaling factors directly, mathematical singularities appear at various angles and combinations of angles, including zero rotation and zero skew. However, the ratios b/a and d/e are well-behaved, being free of all such singularities in the domain of interest.

First, define the ratios r_1 and r_2:

$$r_1 = \frac{b}{a} = \frac{\sin(\theta - \phi)}{\cos\theta} \text{ and } r_2 = \frac{d}{e} = \frac{\sin\theta}{\cos(\theta - \phi)} \tag{B.11}$$

Then square the ratios:

$$r_1^2 = \frac{\sin^2(\theta - \phi)}{\cos^2\theta} \text{ and } r_2^2 = \frac{\sin^2\theta}{\cos^2(\theta - \phi)} \tag{B.12}$$

Define the intermediate variables X, $(1-X)$, Y and $(Y-1)$:

$$X = \cos^2(\theta), Y = \cos^2(\theta - \phi); (1 - X) = \sin^2(\theta), (1 - Y) = \sin^2(\theta - \phi) \tag{B.13}$$

The ratios may now be expressed as functions of these intermediate variables:

$$r_1^2 = \frac{1-Y}{X} \text{ and } r_2^2 = \frac{1-X}{Y} \tag{B.14}$$

Solve for X and Y:

$$X = \frac{r_2^2 - 1}{r_1^2 r_2^2 - 1} \text{ and } Y = \frac{r_1^2 - 1}{r_1^2 r_2^2 - 1} \tag{B.15}$$

In theory, X and Y cannot be less than zero or more than unity. In practice, when computed from measured data, X and Y may nonetheless very slightly exceed this range.

The excess over unity will never be more than slight because even with large errors in measurement of the point locations in object space, there is always a set of rotation and skew angles plus scale factors that allow one to transform between object and image spaces. The effect of measurement errors is therefore to cause proportionate errors in the resulting pure scaling factors, but the X and Y values will never significantly exceed unity. The remaining very slight excess over unity is therefore harmless in the present algorithm, and so will be ignored.

The less-than-zero case is covered by requiring X and Y to exceed specified minimum values. If $X \leq \cos^2(5°)$, the rotation angle is too large. Likewise, if $Y \leq \cos^2(10°)$, the skew angle is too high. The limits in the two cosines differ because the worst case for Y is when rotation and skew angles have different signs, while X depends only on the rotation angle. The mathematical limit is closer to 40 °, where 1/cos() becomes too large and too noisy to support the desired accuracy.

Given the two intermediate variables X and Y, the inverses of the pure scaling factors may be computed as follows:

$$M_x = \frac{a}{\sqrt{X}} \text{ and } M_y = \frac{e}{\sqrt{Y}} \tag{B.16}$$

And then we compute the pure scaling factors:

$$S_x = \frac{1}{M_x} \text{ and } S_y = \frac{1}{M_y} \tag{B.17}$$

This concludes the derivation. The procedure is described in normative Annex C.

Annex C
(normative)

Procedure for geometric calibration using the micropositioner

Step 1. Collect object and image locations of three points. This is accomplished by illuminating the fibre with a calibration light source (see 5.1.9), and using the micropositioner to move the fibre in the object XY plane to three well-separated non-collinear positions, just inside the image frame borders. At each position, the X and Y coordinate settings of the stage is recorded and an image is captured. In each image, the centroid of flux exceeding a threshold is computed and used as the corresponding position in image space.

For accuracy, all of the positions shall be far enough from all edges of the image frame that no above-threshold pixels are clipped by an encroaching frame edge, and all above-threshold intensity values shall be from the linear range of the imager chip.

Also for accuracy, the error in X-coordinate (Y-coordinate) location cannot exceed and ± 1 %. In other words, if X-coordinate length of the smallest axis-aligned rectangle into which the calibration points fit is 200 µm, the total error in X-coordinate values cannot exceed 200/100= 2 µm. Likewise Y.

The calibration points are identified as p_i (as seen in object space) and p_i' (the same point as seen in image space), where i runs from 1 to 3. The order of numbering the calibration points is not significant.

Step 2. If there are fewer than three calibration points, stop processing and report an "insufficient calibration points" error. Otherwise, continue processing.

Step 3. If any of the calibration points falls too close to any edge of the image frame, stop processing and report a "frame encroachment" error. Otherwise, continue processing.

Step 4. If the intensity of more than 1 % of the valid pixels exceeds 95 % of the maximum possible linear intensity value, stop processing and report a "pixel saturation" error. Otherwise, continue processing.

Step 5. Verify that the calibration points are neither collinear nor too close together by computing the area of the triangle formed by the points, and comparing this area to the area of the image frame containing the points.

Compute the area of the triangle[1]:

$$A_{\text{triangle}} = \frac{1}{2} \text{abs}(\det[P'])$$ (C.1)

where

$P' = \begin{bmatrix} p_1' & p_2' & p_3' \end{bmatrix}$ contains the three calibration points as seen in image space,

---

[1] This formula may be derived from "The Surveyor's Area Formula", Bart Braden, The College Mathematics Journal, September 1986, v.14, n.4, pages 326-337.

$$p_i' = \begin{bmatrix} x_i' \\ y_i' \\ 1 \end{bmatrix}, \det[\ ] \text{ is the determinant, and } abs(\ ) \text{ is the absolute-value function.}$$

If $A_{triangle}$ covers less than 10 % of the area of the image, stop processing and report a "calibration point geometry" error. Otherwise, proceed to next step.

Step 6: Compute the following data matrix:

$$\begin{bmatrix} a & b & c \\ d & e & f \\ q & r & s \end{bmatrix} = P' \times P^{-1} \tag{C.2}$$

where

$$P' = \begin{bmatrix} p_1' & p_2' & p_3' \end{bmatrix} \text{ and } P = \begin{bmatrix} p_1 & p_2 & p_3 \end{bmatrix}$$

$$p_i = \begin{bmatrix} x_i \\ y_i \\ 1 \end{bmatrix} \text{ and } p_i' = \begin{bmatrix} x_i' \\ y_i' \\ 1 \end{bmatrix},$$

Step 7: Verify the assertion that the constants q, r, and s have emerged correctly as {0,0,1}, to within roundoff or numerical error, as a general test on the programming. This test cannot be failed by bad data – a coding or algorithm error is required. Compute the deviation from the expected constant values:

$$C_{err} = abs(q) + abs(r) + abs(1 - s) \tag{C.3}$$

where $abs(\cdot)$ is the absolute-value function.

If C_{err} exceeds 10^{-6}, stop processing and report a fatal "failed constants-value program assertion" error. Otherwise, continue to next step.

Step 8: Compute the intermediate variables X and Y:

First, compute the squared ratios:

$$r_1^2 = \left(\frac{b}{a}\right)^2 \text{ and } r_2^2 = \left(\frac{d}{e}\right)^2 \tag{C.4}$$

Then, compute X and Y from the squared ratios:

$$X = \frac{r_2^2 - 1}{r_1^2 r_2^2 - 1} \text{ and } Y = \frac{r_1^2 - 1}{r_1^2 r_2^2 - 1} \tag{C.5}$$

Step 9: If $X \leq \cos^2(5°)$, report a fatal "rotation angle too large" error and stop processing. Otherwise, proceed to next step.\

Step 10: Likewise, if $Y \leq \cos^2(10°)$, report a fatal "skew angle too large" error and stop processing. Otherwise, proceed to next step.

Step 11: Given the intermediate variables, the pure scaling factors are computed as follows:

$$S_x = \frac{\sqrt{X}}{a} \text{ and } S_y = \frac{\sqrt{Y}}{e} \tag{C.6}$$

Step 12: Return the pure scaling factors S_x and S_y which have units microns per pixel, for use in converting image dimensions into object dimensions.
This completes the procedure.

Bibliography

IEC 60793-1-20 , *Optical fibres – Part 1-20: Measurement methods and test procedures – Fibre geometry*

IEC 60793-1-41, *Optical fibres – Part 1-41: Measurement methods and test procedures – Bandwidth*

IEC 61745:2017, *End-face image analysis procedure for the calibration of optical fibre geometry test sets*

ANSI/EIA-440-B:2004, *Fiber optic terminology*

David F. Rogers and J. Alan Adams, *Mathematical elements for computer graphics*, 2nd edition, McGraw-Hill, 1990

James R. Janesick, *Scientific charge-coupled devices*, SPIE Press, 2001

James R. Janesick, Morely M. Blouke, and J. Freeman, *Scientific charge-coupled devices*, Optical Engineering, August 1987, Vol. 26, No. 8, pp. 692-714

Foley et al, Addison-Wesley, *Computer graphics: principles and practice*, 2nd edition, 1990

Holst, Gerald C., *Electro-optical imaging system performance*, JCD Publishing and SPIE Press, 1995

_____

IEC 61280-1-4

INTERNATIONAL STANDARD

NORME INTERNATIONALE

colour inside

**Fibre optic communication subsystem test procedures –
Part 1-4: General communication subsystems – Light source encircled flux
measurement method**

**Procédures d'essai des sous-systèmes de télécommunication fibroniques –
Partie 1-4: Sous-systèmes généraux de télécommunication – Méthode de
mesure du flux inscrit de la source optique**

CONTENTS

INTERNATIONAL ELECTROTECHNICAL COMMISSION

_____

FIBRE OPTIC COMMUNICATION SUBSYSTEM TEST PROCEDURES –

Part 1-4: General communication subsystems – Light source encircled flux measurement method

FOREWORD

1) The International Electrotechnical Commission (IEC) is a worldwide organization for standardization comprising all national electrotechnical committees (IEC National Committees). The object of IEC is to promote international co-operation on all questions concerning standardization in the electrical and electronic fields. To this end and in addition to other activities, IEC publishes International Standards, Technical Specifications, Technical Reports, Publicly Available Specifications (PAS) and Guides (hereafter referred to as "IEC Publication(s)"). Their preparation is entrusted to technical committees; any IEC National Committee interested in the subject dealt with may participate in this preparatory work. International, governmental and non-governmental organizations liaising with the IEC also participate in this preparation. IEC collaborates closely with the International Organization for Standardization (ISO) in accordance with conditions determined by agreement between the two organizations.

2) The formal decisions or agreements of IEC on technical matters express, as nearly as possible, an international consensus of opinion on the relevant subjects since each technical committee has representation from all interested IEC National Committees.

3) IEC Publications have the form of recommendations for international use and are accepted by IEC National Committees in that sense. While all reasonable efforts are made to ensure that the technical content of IEC Publications is accurate, IEC cannot be held responsible for the way in which they are used or for any misinterpretation by any end user.

4) In order to promote international uniformity, IEC National Committees undertake to apply IEC Publications transparently to the maximum extent possible in their national and regional publications. Any divergence between any IEC Publication and the corresponding national or regional publication shall be clearly indicated in the latter.

5) IEC itself does not provide any attestation of conformity. Independent certification bodies provide conformity assessment services and, in some areas, access to IEC marks of conformity. IEC is not responsible for any services carried out by independent certification bodies.

6) All users should ensure that they have the latest edition of this publication.

7) No liability shall attach to IEC or its directors, employees, servants or agents including individual experts and members of its technical committees and IEC National Committees for any personal injury, property damage or other damage of any nature whatsoever, whether direct or indirect, or for costs (including legal fees) and expenses arising out of the publication, use of, or reliance upon, this IEC Publication or any other IEC Publications.

8) Attention is drawn to the Normative references cited in this publication. Use of the referenced publications is indispensable for the correct application of this publication.

9) Attention is drawn to the possibility that some of the elements of this IEC Publication may be the subject of patent rights. IEC shall not be held responsible for identifying any or all such patent rights.

IEC 61280-1-4 has been prepared by subcommittee 86C: Fibre optic systems and active devices, of IEC technical committee 86: Fibre optics. It is an International Standard.

This third edition cancels and replaces the second edition published in 2009. This edition constitutes a technical revision.

This edition includes the following significant technical changes with respect to the previous edition:

a) improvement of calibration procedure and calibration traceability;

b) improvement of fibre shaker description and requirements;

c) addition of pulsed light sources;

d) removal of a poorly traceable calibration process using a micro positioner.

The text of this International Standard is based on the following documents:

Draft	Report on voting
86C/1806/CDV	86C/1828/RVC

Full information on the voting for its approval can be found in the report on voting indicated in the above table.

The language used for the development of this International Standard is English.

This document was drafted in accordance with ISO/IEC Directives, Part 2, and developed in accordance with ISO/IEC Directives, Part 1 and ISO/IEC Directives, IEC Supplement, available at www.iec.ch/members_experts/refdocs. The main document types developed by IEC are described in greater detail at www.iec.ch/publications.

A list of all parts of the IEC 61280 series can be found, under the general title *Fibre optic communication subsystem test procedures*, on the IEC website.

The committee has decided that the contents of this document will remain unchanged until the stability date indicated on the IEC website under webstore.iec.ch in the data related to the specific document. At this date, the document will be

- reconfirmed,
- withdrawn,
- replaced by a revised edition, or
- amended.

IMPORTANT – The "colour inside" logo on the cover page of this document indicates that it contains colours which are considered to be useful for the correct understanding of its contents. Users should therefore print this document using a colour printer.

INTRODUCTION

This part of IEC 61280 specifies how to measure the encircled flux of a multimode light source. Encircled flux is a fraction of the cumulative output power to the total output power as a function of radial distance from the centre of the multimode optical fibre's core.

The basic approach is to collect two-dimensional (2D) nearfield data, using a calibrated camera, and to mathematically convert the 2D data into three normalized functions of radial distance from the fibre's optical centre. The three functions are intensity, incremental flux, and encircled flux. The intensity represents optical power per surface area (in watts per square meter). The incremental flux represents optical power per radius differential (in watts per meter), and the encircled flux represents a fraction of the cumulative output power to the total output power.

These three radial functions are intended to characterize fibre optic laser sources either for use in mathematical models predicting the minimum guaranteed length of a communications link, or to qualify a light source to measure insertion loss in multimode links.

FIBRE OPTIC COMMUNICATION SUBSYSTEM
TEST PROCEDURES –

Part 1-4: General communication subsystems –
Light source encircled flux measurement method

1 Scope

This part of IEC 61280 establishes the characterization process of the encircled flux measurement method of light sources intended to be used with multimode fibre.

This document sets forth a procedure for the collection of two-dimensional fibre optic nearfield greyscale data and subsequent reduction to one-dimensional data expressed as a set of three sampled parametric functions of radius from the fibre's optical centre.

Estimation of the fibre core diameter is not an objective of this document.

2 Normative references

The following documents are referred to in the text in such a way that some or all of their content constitutes requirements of this document. For dated references, only the edition cited applies. For undated references, the latest edition of the referenced document (including any amendments) applies.

IEC 60793-2-10, *Optical fibres – Part 2-10: Product specifications – Sectional specification for category A1 multimode fibres*

IEC 60825-1, *Safety of laser products – Part 1: Equipment classification and requirements*

3 Terms and definitions

For the purposes of this document, the following terms and definitions apply.

ISO and IEC maintain terminology databases for use in standardization at the following addresses:

- IEC Electropedia: available at https://www.electropedia.org/
- ISO Online browsing platform: available at https://www.iso.org/obp

3.1
calibration light source
light source used to find the optical centre of a multimode fibre

3.2
centroid image
image used to determine the optical centre of the multimode fibre core

3.3
corrected image
image which has had a dark image subtracted from it and whose elements have had uniformity correction applied

3.4
dark image
image taken with the measured light source either turned off or not installed in the input port

Note 1 to entry: Stray light and electrical signals of the detection system will remain in the dark image.

3.5
image
two-dimensional rectangular array of numbers whose elements are pixels and whose pixel values linearly correspond to the optical power falling on the pixels

3.6
light source
something that emits light that is coupled into a fibre, the output of which can be measured

EXAMPLE   Calibration light source, transmission light source, light source used for attenuation measurements.

3.7
measurement light source
light source intended to be used in the measurement of attenuation

3.8
nominal core radius
half the nominal core diameter of the multimode fibre to be measured

3.9
ring smoothing
technique to reduce the two dimensional near field image into a 1-D near field intensity profile while cancelling the effects of the periodic spacing of imager pixels of finite area

3.10
transmission light source
light source used to transmit digital data over multimode fibre optic links

3.11
uniformity correction
process to correct the sensitivity of a pixel so that it performs substantially like an average pixel

3.12
valid pixel
optical detection element in the detector matrix whose sensitivity, when corrected, is within 5 % of the mean sensitivity of the average conversion efficiency of the detector

4   Symbols

B baseline intensity

> NOTE 1   This value is determined from a region of the computed near field just outside the core boundary.

D distance from the centre of the centroid image to the nearest boundary of the image

D_L, D_R, D_T, D_B set of distances from the centre of the centroid image to, respectively, the left, right, top and bottom boundaries of the image

> NOTE 2   The minimum of this set is used to compute D.

$EF(i)$ encircled flux vector

$EF'(i)$ non-normalized encircled flux vector

i	index parameter used in the parametric result vectors and $EF(i)$
I_{dark}	matrix of pixel intensities of a dark image as measured by the detector and digitizer
I_{raw}	matrix of pixel intensities of the light source, before correction, as measured by the detector and image digitizer
$I_{r,c}$	near-field intensity matrix
	NOTE 3 This is a matrix of pixel intensities, based on I_{raw}, as measured by the detector and corrected using U and I_{dark}.
$I(i)$	ring-smoothed intensity vector, each element being the arithmetic average of the set of radial coordinates of all the pixels in a given ring
N_R	number of rings used to compute the 1-D near field
N_r	number of rows in an image
	NOTE 4 All columns in an image have the same number of rows.
N_c	number of columns in an image
	NOTE 5 All rows in an image have the same number of columns.
P_{Max}	most intense valid pixel in the centroid image
P_{Min}	least intense valid pixel in the centroid image
R	radial coordinate, in µm, of the centre of any pixel, referenced to the optical centre X_0, Y_0
$R(i)$	ring-smoothed radial vector, each element being the arithmetic average of the radii of all the pixels in the ith ring
R_{max}	integration limit along the radius
S_c	column-weighted summation of all pixel intensities greater than T in the centroid image
$S_I(i)$	intensity summation vector used in ring smoothing
S_P	summation of all pixel intensities greater than T in the centroid image
$S_N(i)$	pixel counting vector used in ring smoothing
$S_R(i)$	radius summation vector used in ring smoothing
S_r	row-weighted summation of all pixel intensities greater than T in the centroid image
S_x	horizontal geometric calibration factor (along columns)
S_Y	vertical geometric calibration factor (along rows)
T	threshold used to determine which pixels in the centroid image will be used to determine the optical centre
	NOTE 6 All pixels greater than or equal to T are used to compute the centroid.
$U_{r,c}$	sensitivity correction matrix, applied to a dark-subtracted image to reduce non-uniformity of the detector's pixel-to-pixel conversion efficiency
W	half-width, in µm, of the rings used to compute the 1-D near field
X_0	X axis (column) location of the centre of the centroid image
Y_0	Y axis (row) location of the centre of the centroid image

5 Assumptions

5.1 Assumptions applicable to the characterization of data sources

The 50 µm or 62,5 µm core near-parabolic graded-index multimode fibre used as the "test jumper assembly" is treated as if it possessed perfect circular symmetry about its optical centre, because asymmetries in the launched optical flux distributions will dominate any distortions introduced by the test jumper assembly, such as lateral and angular misalignments. It is further assumed that all cladding modes will be stripped by passage through the specified ten metres or more of fibre. The modes of a mode group need not carry equal flux. In fact, with such short fibres, one thousand metres or less, unequal distribution of flux in the modes of a group is the norm, not the exception.

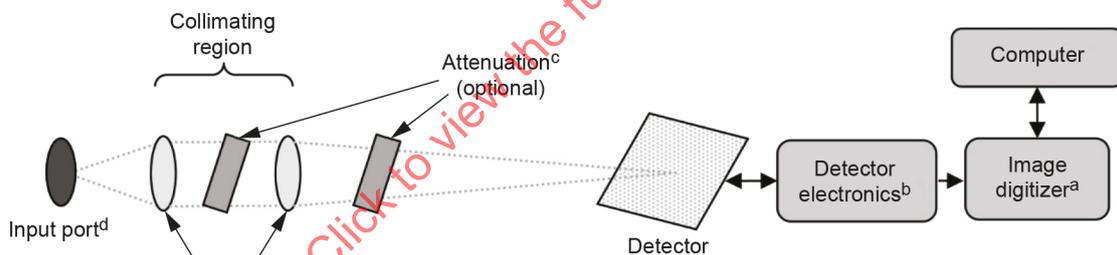### 5.2 Assumptions applicable to the characterization of measurement sources

Measurement sources are assumed to be sufficiently broadband and incoherent, so that speckle is not a problem, and to have a sufficiently symmetrical nearfield distribution, so that the truncated centroid of that nearfield indicates the location of the optical centre of the fibre with sufficient accuracy for the purposes of this document.

6 Apparatus

6.1 Common apparatus

6.1.1 General

Figure 1 below shows an apparatus block diagram.

a The image digitizer can be either part of a camera or a computer add-in board.

b The detector electronics are usually integral to the camera and digitizer.

c Attenuation is best placed in the collimating region of the optical path, but not all optical designs will have an accessible collimating region. When this is not possible, the attenuation should be placed on the detector side of the optics.

d When a micro positioner (not shown) is employed, the input port will be physically attached to it.

Figure 1 – Apparatus block diagram

6.1.2 Computer

A computer is required, because the acquired image contains many thousands of pixels, and the reduction of the image to encircled flux requires substantial computation. The computer will usually be connected to the image digitizer to control the acquisition of an image through software and can also control the micro positioner (and the source, if correlated double sampling is implemented).

6.1.3 Image digitizer

The nearfield of the fibre core is imaged onto the detector and then digitized by the image digitizer. The image digitizer can be an integral part of a camera, which also contains the detector, or can be an add-in frame-grabber board in the computer.

Automatic circuitry in the digitizer, for example automatic gain control (ABC) often found in video cameras, shall be disabled.

6.1.4 Detector

The detector is typically a charge-coupled device (CCD) or complementary metal-oxide semiconductor (CMOS) camera. Other types of array cameras can be considered. In any case, detectors shall be both nominally linear and memoryless. Absolute radiometric measurement of flux (optical power flow) is not required.

Automatic circuitry in the detector, for example automatic gain control often found in video cameras, shall be disabled.

The difference in conversion sensitivity from pixel to pixel in the detector will affect the measurement accuracy. The non-uniformity in the corrected conversion efficiency of the detector shall not exceed ±5 %. It is possible to calibrate and correct a detector, whose uncorrected uniformity is worse than 5 %, by applying a pixel-by-pixel sensitivity correction matrix, U, to the raw image. Often, this correction is part of the camera function (and so each element of U can be taken as unity). Sometimes, the correction matrix can be provided by the detector supplier. In other cases, the correction matrix shall be determined by the procedure outlined in Clause A.2.

Detectors can have invalid pixels, which are pixels whose corrected conversion efficiency exceeds ±5 % of the average conversion efficiency of the detector. Invalid pixels will often produce no signal, a completely saturated signal, or be stuck at some intermediate value. Detectors whose invalid pixel count exceeds 0,1 % of the total number of pixels shall be rejected.

In most cameras and image digitizers, the setting of the "black level" is user adjustable. Since the detector will be slightly noisy, it is important that the detector and digitizer do not clip random black signals at zero (in common systems, random noise in a detector will have a standard deviation less than 0,5 % of the saturation level). To ensure no clipping of the noise, when settable, set the black level to produce a small positive signal (typically at least five times the standard deviation of the noise) when no light is impinging on the detector.

6.1.5 Magnifying optics

Suitable optics shall be provided to project the magnified image of the input port onto the detector, in such a way that the detector can measure the entire nearfield flux distribution. The numerical aperture of the magnifying optics shall exceed the nominal numerical aperture of the fibres (as specified in the fibre's family specification) used in calibration or measurement. Microscope objectives are often appropriate for this purpose.

NOTE   When a microscope objective is used, its actual magnification as used in the present apparatus generally will not be the same as the nominal magnification factor engraved into the side of the objective, because the present apparatus differs from the standard microscope for which that nominal magnification factor was computed. The geometric calibration procedures outlined in Clause 8 determine the actual magnification.

Reflections from optical surfaces can seriously degrade the measurement of encircled flux. Anti-reflection coating at the wavelength of measurement or other forms of reflection control can be considered to reduce reflections.

Measurement precision is important when characterizing measurement light sources, so that optical distortion is kept to a minimum. Careful selection and application of the lenses and other

optical components is recommended. Plan-type microscope objectives are an example of suitable optics. The procedures found in IEC 61745:2017 can be used to assess the optical integrity of the apparatus.

It is important that the distance between the detector and all elements of the magnifying optics be held fixed once calibration is performed. When the relationship between these elements changes, the magnification is expected to change enough that recalibration will be required. Focusing shall be accomplished by changing only the distance between input port and the magnifying optics.

6.1.6   Attenuator

Often, the optical flux of the source will saturate the detector and the only effective solution is to employ optical attenuation. Any attenuation element shall not reduce the numerical aperture of the optical system and shall not be the source of significant reflections or optical distortions, which will bias the resulting encircled flux.

NOTE 1   When neutral density filters are used in the optical system, geometric distortions can be introduced.

NOTE 2   Changing the attenuation between the optical centre image and the image of the measured source can cause the location of the optical centre of the measurement source to move away from that determined using the optical centre image, causing errors in the resulting radial data functions.

6.1.7   Micro positioner (optional)

The micro positioner is an optional part of the apparatus. Depending on the apparatus design, it is possible to rely on connector ferrule geometry to place the image completely onto the detector without a micro positioner. In many implementations, only a focus adjustment (Z axis) is necessary, and in some cases, all three axes may only require alignment during construction or maintenance of the apparatus. Using the ferrule to place the fibre core image onto the detector does not relieve the requirement of finding the optical centre as required by 9.3.

When used, the purpose of the micro positioner is to bring the projected image of the fibre face into focus on the detector and to determine the magnification of the apparatus (see Clause 8). Mechanical locking mechanisms or their equivalents are required for all three axes to prevent mechanical drift during measurement. The micro positioner can optionally be driven by motors and can optionally employ feedback mechanisms to control the actual position of the stage (and thus the fibre face).

6.1.8   Input port

The input port is where the calibration artefacts and measurement samples are connected to the apparatus. The input port characteristics depend on which type of source is to be characterized.

When characterizing transmission light sources, the input port is the distal end of the test jumper assembly. The proximal end of the test jumper assembly will be imaged onto the detector. When a micro positioner is used, the proximal end will be attached to the micro positioner.

When characterizing measurement light sources, the input port is commonly a connector bulkhead or its equivalent. When a micro positioner is employed, the bulkhead will be attached to the micro positioner.

See 6.2 and 6.3 for particular requirements.

6.1.9   Calibration light source

The calibration light source is used when calibrating the apparatus (see Clause 8). When this source is used to illuminate the test jumper assembly, the calibration source shall overfill the modes of the jumper. Optionally, a mode scrambler can be used with the chosen calibration

source to ensure more uniform overfilling of the fibre. See IEC 60793-1-41 for information on mode scramblers.

Any spectrally broad non-coherent light source, such as a tungsten-halogen lamp, a xenon arc lamp, or a light-emitting diode (LED), can be used to overfill the fibre of the test jumper assembly. When calibrating the apparatus for the characterization of measurement light sources, the centre wavelength of the calibration source shall be within 30 nm of the nominal wavelength of the light sources to be qualified, and its spectral width (i.e., full width at half maximum) shall be no more than 100 nm. When calibrating the apparatus for the characterization of transmission light sources, the spectral characteristics of the calibration source are not specified, but it is recommended that its spectrum be similar to the sources to be characterized. The chosen calibration source shall be stable in intensity over a time period sufficient to perform the measurements.

6.2 Transmission source apparatus

6.2.1 General

When characterizing transmission light sources, the input port of the apparatus consists of two elements, the test jumper assembly and the fibre shaker (see Figure 2 below).
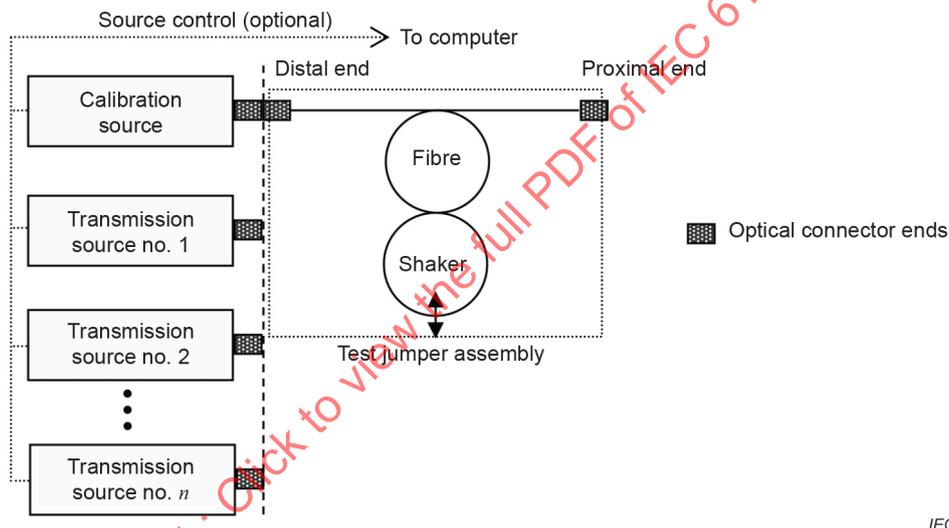

Figure 2 – Typical set-up for transmission source measurement

6.2.2 Test jumper assembly

The purpose of the test jumper assembly is to strip cladding modes, and to allow speckle to be averaged out by mechanical flexing of a portion of the test jumper assembly. The test jumper assembly is used only when qualifying light sources for multimode transmission.

The test jumper assembly shall be at least 10 m in length, made of germanium-doped near-parabolic graded-index fused-silica multimode "glass", an IEC 60793-2-10 class A1-OM2 to OM5 fibre with a core diameter of 50 μm or class A1-OM1 fibre with a core diameter 62,5 μm. The test jumper assembly shall consist of a single, uncut length of fibre with connectors at each end. The test jumper assembly connectors shall have single-mode mechanical tolerances, even though the fibre is multimode.
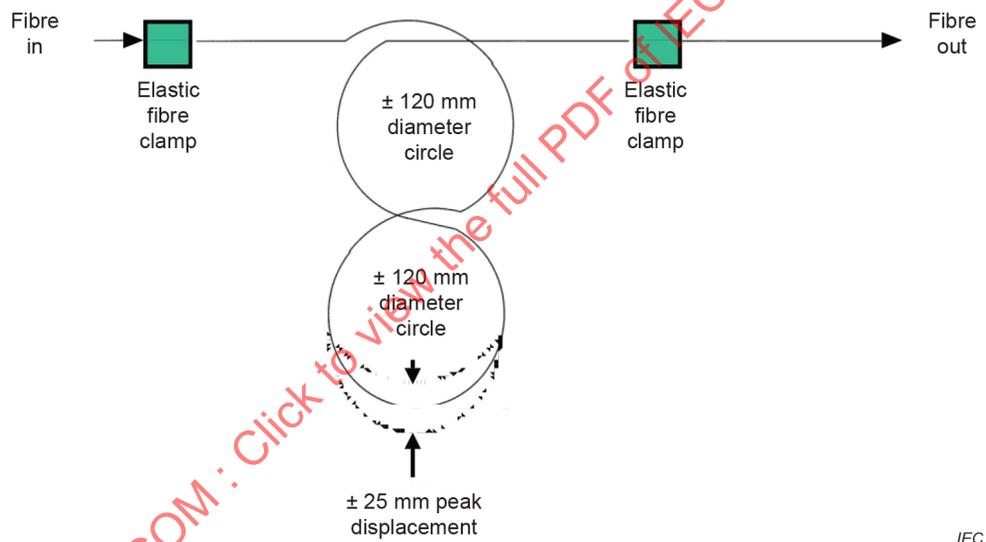
6.2.3 Fibre shaker

The purpose of the fibre shaker is to change the differential path length of the various modes in the test jumper, ensuring that speckle in the averaged image will be reduced, as the image is averaged. Speckle reduction can be accomplished in a variety of ways and shall be good

enough to ensure sufficient repeatability in the measurement of encircled flux. Shaking of the test jumper assembly with a mechanical device is required to reduce speckle.

Part of the test jumper assembly shall be mechanically shaken continuously in each of three nominally orthogonal directions (using three independent shaker mechanisms) during the measurement, making at least one hundred shake cycles in each of the three directions during the measurement period. The shake frequencies in the three directions shall be chosen such that the three shake cycles synchronize no more often than once every five hundred cycles of the middle shake frequency.

A fibre shaker mechanism can be of any design as long as it induces large amplitude movements and flexing in the optical fibre. Fibre transverse displacements of more than 25 mm are suggested. The fibre shakers shall include a fibre holding fixture for securely holding the fibre.

One exemplary mechanism, shown in Figure 3, has three turns of fibre coiled into a 3-ply figure-eight arrangement, with the loops each being approximately 120 mm in diameter. A motor-driven eccentric drives a slider back and forth at about one stroke per second, alternately flattening and stretching one loop of the figure eight with 25-mm amplitude. Three such mechanisms in series will consume about $3 \times 3 \times (2 \times \pi \times 0,120) = 6,8$ m of the test jumper assembly's fibre.

NOTE 1   Only one figure-eight loop of the three loops is shown here, for visual clarity. Fibre clips are used to keep fibre in place, in addition to elastic fibre clamps that prevent transmission of fibre motion. Loose fibre clips not shown.

NOTE 2   Fibre is moved back and forth as shown, with a peak-to-peak amplitude of about 25 mm, distorting one fibre loop.

Figure 3 – Fibre shaker example

Another exemplary approach is to hang large loose loops of fibre in front of a large fan which blows these loops about, the turbulence in the stream of the fan randomizing the motion.

NOTE 1   The fibre ends leading into and out of the fibre shakers are mechanically fixed or stabilized to prevent movement of fibres at connection points. In addition, the fibre shakers are mechanically isolated from the rest of the test setup so that vibrations are not transmitted to connection points throughout the apparatus, or to the micro positioner, detector, or magnifying optics. Vibration reduction is easier if the fibre shaker is both statically and dynamically balanced, and if all moving components are light in weight.

NOTE 2   There is no required relation between the measurement period (containing the one hundred strokes) and the acquisition time of an image. Typically, in each measurement period, many individual images are taken and later summed or averaged by the computer; this technique can help to avoid detector saturation. The detector and digitizer can perform an equivalent function independently. The image will be relatively speckle free when one hundred shake cycles are averaged in this way.

6.3   Measurement source apparatus

The apparatus as described in 6.1 is sufficient to characterize measurement light sources. Fibre shaking or other speckle reduction techniques shall not be employed.

NOTE   This document does not address the characterization of OTDR transmitters, which will display significant speckle. At the time of publication of this document, the characterization of encircled flux for OTDRs was still under study.

7   Sampling and specimens

Light sources to be tested shall be chosen and prepared as defined by the user of this document, who shall document the sampling and preparation procedures used. The only requirements on the light sources under test are that they have an operating wavelength compatible with the detector and have optical connectors or splices compatible with the input port of the apparatus. The construction details of the light sources are otherwise unspecified.

When qualifying lasers, the laser drive current shall be sufficient to ensure that the laser always acts as a laser, rather than as a light-emitting diode (LED).

8   Geometric calibration

Calibration of the apparatus is critical to the accuracy of this measurement procedure (see Clause A.4 for a description of the kinds of noise and errors that calibration can correct). Calibration shall be performed periodically and should be performed at least monthly. If the calibration is known to drift significantly during a measurement interval, the source(s) of the drift shall be identified and eliminated. If the apparatus is disassembled, or its components in the optical path or affecting the optical path are otherwise manipulated, calibration shall be performed before measurements are made.

The purpose of geometric calibration is to obtain the measurement data needed to compute the magnification factors S_X and S_Y which have units of microns per pixel. These factors will be used to convert camera coordinates to fibre end-face coordinates. These magnification factors can be arrived at by using IEC 61745:2017 (specifically 5.3.4.2).

9   Measurement procedure

9.1   Safety

All procedures in which an LED or laser source is used as the optical source shall be carried out using safety precautions in accordance with IEC 60825-1.

9.2   Image acquisition

9.2.1   Raw image acquisition

9.2.1.1   General

Acquiring an image is central to the measurement of encircled flux. The approach to image acquisition depends on the general characteristics of the light source being measured. When acquiring transmission light source images, a fibre shaker is required, which in turn requires that some form of averaging be performed.

Measurements of light sources, on the other hand, will not require a fibre shaker, and usually their optical intensity is sufficient to allow very short detector integration times. These issues are discussed in 9.2.1.2 and 9.2.1.3.

In any case, the raw image obtained from the measurements described in 9.2.1.2 and 9.2.1.3 is a matrix of uncorrected intensities I_{raw}, whose dimensions are N_r rows by N_c columns.

9.2.1.2 Transmission light source image acquisition

Since transmission light sources require a fibre shaker, and the resultant image shall be integrated over at least 100 cycles of the fibre shaker, long integration times are required. Direct detector integration and digital image accumulation can be employed to achieve the required integration. A typical procedure is to acquire multiple frames and sum or average them numerically, pixel-by-pixel. This approach prevents detector saturation while integrating enough shaker cycles to effectively reduce speckle.

9.2.1.3 Measurement light source image acquisition

Typical measurement light sources require only one short-period detector integration to arrive at a usable raw image. These sources are sufficiently incoherent and are sufficiently intense to easily get adequate dynamic range, although attenuation may be required to operate the detector within its linear range.

NOTE   OTDR measurement light sources present significant challenges to applying this method and have not been investigated.

9.2.2 Dark image acquisition

The dark image is used to correct the raw image, pixel-by-pixel, for dark currents and DC offsets introduced by the detector and digitizer. To acquire the dark image, the detector integration time and digital image accumulation shall be the same as was used to acquire I_{raw}. The dark image is acquired with the input port of the apparatus blocked to prevent light from entering the optical system. The resultant image is the matrix I_{dark}.

In some systems, the dark image is sufficiently uniform to be assumed constant for all pixels. In this case, each element of I_{dark} can be taken as zero. The average dark level will be removed from the resultant data by the baseline subtraction procedure outlined in 10.2.

9.2.3 Corrected image

The corrected image matrix I, is computed from the matrices I_{raw}, I_{dark} and $U_{r,c}$ as shown in Formula (1).

$$I_{r,c} = \left(I_{raw_{r,c}} - I_{dark_{r,c}} \right) * U_{r,c} \tag{1}$$

where

$U_{r,c}$ is the sensitivity correction matrix, reducing non-uniformity of the detector's pixel-to-pixel conversion efficiency.

NOTE 1   The asterisk (*) operator denotes element-by-element multiplication.

NOTE 2   When the camera is sufficiently uniform without correction, and the baseline subtraction step of 10.2 is to be performed, no correction is required, so I can be set to I_{raw}.

9.3 Optical centre determination

9.3.1 General

Encircled flux is computed with respect to the optical centre of the multimode fibre's core. It is known that coherent light sources can produce, at least over short distances, near fields which are not symmetric about the centre of the fibre core. When measuring transmission sources,

which are typically coherent, the optical centre of the test jumper assembly cannot be determined from the nearfield image of the transmission light source itself. Instead, the test jumper assembly's centre is determined by illuminating its core with a calibration source and finding the centroid of the resulting nearfield.

Since transmission light sources require two separate images to make a measurement of encircled flux (i.e., the image for centring and an image of the light source to be measured), attenuation setting is more challenging. As previously noted, moving or changing the attenuation between two images can shift the optical centre of the image. It is recommended that one attenuator setting be used for both images.

9.3.2   Centroid image

The centroid image is the image used to determine the optical centre of the multimode fibre cord. As discussed above, the centroid image for transmission light sources is an image of the test jumper assembly illuminated by a calibration light source. For measurement light sources, the same image shall be used to find both the optical centre of the fibre and to compute the encircled flux. Use 9.1 to acquire the centroid image.

NOTE   A transmission light source centroid image can be used for any number of measurements of encircled flux as long as the test jumper assembly's optical centre is sufficiently stable with respect to the detector. Stability of the micro positioner, if used, and reasonable control of the ambient environment help ensure that the test jumper remains fixed in place.

9.3.3   Centroid computation

Using the centroid image, the near field centre is computed by finding the centre of gravity of the light intensity distribution for each Cartesian axis independently.

To find the centroid, first find P_{Max} and P_{Min}, which are the intensities of the brightest and dimmest valid pixels in the entire centroid image (using invalid pixels will corrupt the determination of T), and then compute the threshold T as shown in Formula (2).

$$T = 0{,}1 \left(P_{\text{Max}} - P_{\text{Min}} \right) + P_{\text{Min}} \tag{2}$$

Next, compute the three summations shown in Formula (3) over all pixels, excluding pixels with intensities less than T, over the row and column indices r and c.

$$
\begin{aligned}
S_{\text{P}} &= \sum_{r=1}^{N_{\text{R}}} \sum_{c=1}^{N_{\text{C}}} \begin{cases} 0 & I(r,c) < T \\ I(r,c) & I(r,c) \geq T \end{cases} \\[2mm]
S_{\text{r}} &= \sum_{r=1}^{N_{\text{R}}} \sum_{c=1}^{N_{\text{C}}} \begin{cases} 0 & I(r,c) < T \\ r\,I(r,c) & I(r,c) \geq T \end{cases} \\[2mm]
S_{\text{c}} &= \sum_{r=1}^{N_{\text{R}}} \sum_{c=1}^{N_{\text{C}}} \begin{cases} 0 & I(r,c) < T \\ c\,I(r,c) & I(r,c) \geq T \end{cases}
\end{aligned}
\tag{3}
$$

Finally, compute the coordinates of the centroid, (X_0, Y_0), as shown in Formula (4).

$$X_0 = \frac{S_c}{S_P}$$

$$Y_0 = \frac{S_r}{S_P}$$
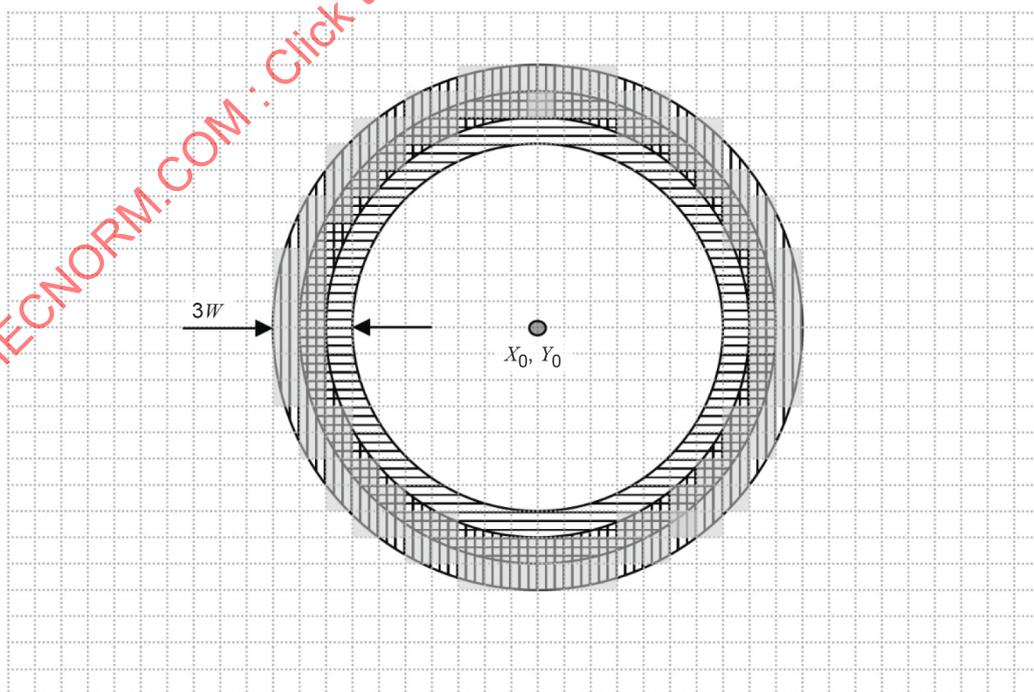
(4)

9.4 Test source image acquisition

To acquire an image of the test source, connect the test source to the apparatus and energize the test source. Allow the test source to warm up as required, and then acquire an image of the test source using the guidelines in 9.1.

10 Computation of encircled flux

10.1 Computation of radial data functions

The first computation step reduces the 2D pixel data into a one-dimensional (1D) radial function by averaging the pixels in sets of nested and overlapping annular rings of thickness $2W$ (where W is 0,2 µm unless otherwise specified), which are centred on the optical centre of the fibre, X_0, Y_0, as defined in 9.3.3. The spacing of the rings is W microns, although the ring's radial coordinate in the resulting radial data functions will be the radial centroid of the radial coordinates of the pixels in the ring.

The filtering concept is illustrated in Figure 4. The elements of the square grid are the pixels of the image. Two rings, centred on the optical centre X_0, Y_0, are shown: the outer ring is hatched vertically, and the inner ring is hatched horizontally. Each ring has a width $2W$ and overlap in a region W wide. The overlap region in the diagram is cross-hatched. The greyed-in pixels are the pixels which will be averaged into the outer ring since their centres fall inside the outer ring's boundary.

Figure 4 – Pixel and ring illustration

Use the following steps to compute the radial functions.

a) Determine the maximum radius of a complete ring. This step finds the largest ring that will fit in the image without being truncated by an image boundary. Compute the shortest distance to the edge of the image from the image centre using Formula (5).

$$
\begin{aligned}
D_L &= S_X X_0 \\
D_R &= S_X \left(N_C - X_0 \right) \\
D_T &= S_Y Y_0 \\
D_B &= S_Y \left(N_R - Y_0 \right) \\
D &= \min \left(D_L, D_R, D_T, D_B \right)
\end{aligned}
\tag{5}
$$

Where the function "min" finds the minimum of the four distances. Next, compute the number of rings, N_R, as shown in Formula (6).

$$
N_R = \frac{D - W}{W}
\tag{6}
$$

b) Allocate and zero the three summation arrays, $S_R(0..N_R)$, $S_I(0..N_R)$, and $S_N(0..N_R)$.

For each and every pixel (on row r and column c), perform the following steps.

c) Compute the radial coordinate R as shown in Formula (7).

$$
R = \sqrt{S_Y^2 \left(r - Y_0 \right)^2 + S_X^2 \left(c - X_0 \right)^2}
\tag{7}
$$

d) Compute the ring index i as shown in Formula (8).

$$
i = \text{trunc} \left(\frac{R}{W} \right) + 1
\tag{8}
$$

e) If i is less than or equal to N_R, then sum into both ring i and ring $i - 1$, as shown in Formulae (9) and (10).

$$
\begin{aligned}
S_R(i) &= S_R(i) + R \\
S_I(i) &= S_I(i) + I(r,c) \\
S_N(i) &= S_N(i) + 1
\end{aligned}
\tag{9}
$$

$$
\begin{aligned}
S_R(i-1) &= S_R(i-1) + R \\
S_I(i-1) &= S_I(i-1) + I(r,c) \\
S_N(i-1) &= S_N(i-1) + 1
\end{aligned}
\tag{10}
$$

The above double sum implements the overlapping-ring smoother.

f) Finally, compute the parametric function pair (where i is the parameter) for each ring by computing the average radius $\overline{R}$ and average intensity $\overline{I'}$ in each ring as shown in Formula (11).

$$\overline{R}(i) = \frac{S_\text{R}(i)}{S_\text{N}(i)}$$

$$\overline{I'}(i) = \frac{S_\text{I}(i)}{S_\text{N}(i)}$$
(11)

Depending on the camera's resolution and the ring thickness selected, it is possible for some of the interior rings to contain no pixels, so the corresponding S_N values will be zero. In this case, the ring should be omitted, the subsequent array elements should be shifted up, and N_R should be decremented. It is also possible for two or more adjacent rings to have the same $\overline{R}$ (or trivially identical, say within 0,01 µm). In these cases, the radii and intensities in these adjacent rings should be averaged, and those rings replaced with one ring of averaged $\overline{R}$ and averaged intensity, and N_R should be decremented appropriately.

10.2 Integration limit and baseline determination

10.2.1 Integration limit

The general equation for encircled flux is given by Formula (12).

$$EF(r) = \frac{\displaystyle\int_0^r r'I(r')dr'}{\displaystyle\int_0^\infty r'I(r')dr'}$$
(12)

The measurable nearfield intensity does not extend very far beyond the fibre's core boundary, and so it is justifiable to truncate the denominator integral at a radius somewhere beyond the core. From a measurement perspective, extending the integral far beyond the core only integrates noise and so only increases the noise of the measurement.

The integration limit, R_Max, shall be set to 1,15 times the nominal core radius of the fibre connected to the test source. For example, R_Max would be set to 28,75 for 50 µm fibres. The maximum index, i_Max, can then be found as the index of the first radius in $\overline{R}(i)$ that is greater than or equal to R_Max.

10.2.2 Baseline determination

Determine the average baseline intensity, B, as the average of a set of $\overline{I'}(i)$ nearby, but outside the core's nearfield. The set of points shall include points from R_Max outwards in radius. The limit where averaging shall be terminated, unless otherwise specified, shall be at radii no greater than 1,2 times the nominal core radius of the fibre connected to the light source.

10.2.3 Baseline subtraction

Compute the baseline-subtracted intensity function, $\overline{I}(i)$, as shown in Formula (13).

$$\overline{I}(i) = \overline{I}'(i) - B \qquad 0 \le i \le i_{\text{Max}} \tag{13}$$

10.3 Computation of encircled flux

The computation of encircled flux is done in two steps: first, integrating the radius-weighted radial data function, $\overline{R}(i) \times \overline{I}(i)$, and then normalizing the function to a maximum of unity. This process will produce another parametric function pair, $\overline{R}$ and EF.

To compute the integral, it has been shown that simple summation or rectangular rule integration produce errors of approximately 0,25 %. These errors can easily be avoided by employing higher-order integration methods. Trapezoidal rule integration is shown in Formula (14) (the special case at index zero stems from the fact that the radius-intensity product at zero radius is identical to zero).

$$EF'(i) = \begin{cases} \dfrac{\overline{R}(0)^2 \, \overline{I}(0)}{2} & i = 0 \\ EF'(i-1) + \dfrac{\overline{R}(i)\overline{I}(i) + \overline{R}(i-1)\overline{I}(i-1)}{2} \times \left[\overline{R}(i) - \overline{R}(i-1)\right] & 0 < i \le i_{\text{Max}} \end{cases} \tag{14}$$

The function $EF(i)$ is then computed by normalizing $EF'(i)$ as shown in Formula (15).

$$EF(i) = \frac{EF'(i)}{EF'(i_{\text{Max}})} \tag{15}$$

In many cases, values of encircled flux at radial values other than the discrete values of $\overline{R}$ are required. It is sufficiently accurate to employ linear interpolation to produce these intermediate values.

11 Results

11.1 Information available with each measurement

Report the following with each measurement:

– date and time of measurement;
– identification of source specimen;
– nominal wavelength of source;
– radius and encircled flux at each radius specified in the detail specification, or if not specified, the radii and encircled flux data computed in Clause 10;
– EF as a graph as a function of radius, including any specified template limits.

11.2 Information available upon request

The following information shall be available upon request:

– date of most recent calibration of equipment;
– method of calibration of equipment;

- ring width, W, used in the computations;
- integration limit parameters, R_{Max} and i_{Max};
- original images used in the computations;
- geometric calibration factors, S_X and S_Y;
- derived centre, and if different, the centroid image;
- radial data functions computed in 10.1.

12 Specification information

The detail specification shall specify the following information:

- type of source to be measured;
- sampling requirements, if any;
- criteria to be met by sources;
- any deviations to the procedure that may apply;
- radii at which the EF is to be reported;
- the EF template used to report results.
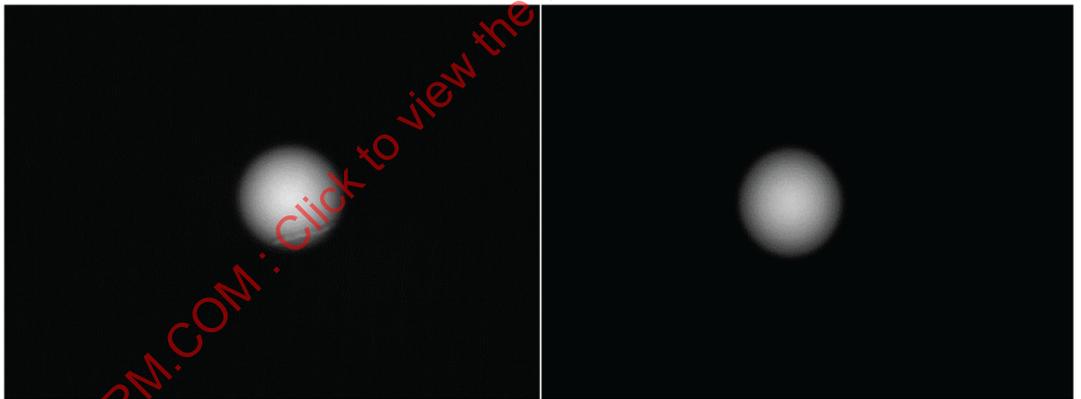
Annex A
(informative)

Measurement sensitivity considerations

A.1   Baseline averaging considerations

A trade-off exists when selecting the region where baseline averaging is performed (see 10.3). The baseline value, B, is subtracted from the entire set of intensities. If the value of B is taken on a single intensity point, then the noise of the system would increase substantially (approximately by the square root of two).

Averaging a region of intensities decreases this noise contribution, if all points in the intensity function have uncorrelated noise. However, imperfections in the optical system of the apparatus, or imperfections in the camera, can make the baseline region outside the core to be non-constant, and so averaging the entire baseline region can cause a bias in B. Selecting an appropriate region over which to make the baseline determination should be done by characterizing the actual apparatus. Clause A.1 provides an analysis of two different images from two different instruments to illustrate methods an instrument designer might use to determine how far baseline averaging should extend into the intensity function.

The two images shown in Figure A.1 below are from two similar instruments (the instruments do not use like components). Both use analogue cameras and PC-integrated frame grabbers, and have similar effective pixel sizes. The images show two different, but similarly filled, 50 μm fibre cores. Instrument A shows a small imperfection on the lower portion of the core, but for this analysis, this imperfection is not important.

IEC

Figure A.1 – Core images from instrument A and instrument B

It is useful to modify the display of the images such that pixels lower than the average background intensity are set to black, and pixels above the average background intensity are set to white, which reveals small non-ideal features in the images. Figure A.2 below shows the two images from Figure A.1 reprocessed in this way.
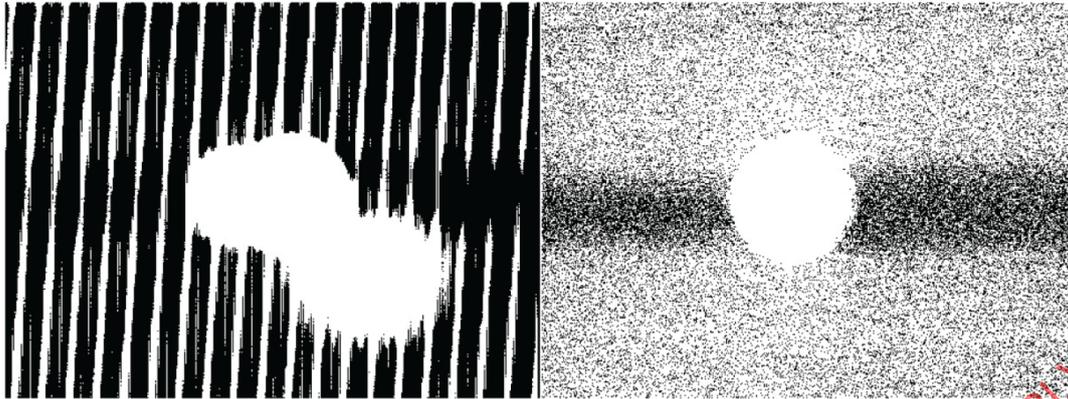
Figure A.2 – Compressed core images from instrument A and instrument B

Instrument A shows a small amount of video pattern noise (the nearly vertical white and dark pattern). Instrument A also shows two white spots not attributable to the core image (to the left and bottom-right of the image). These spots are most probably caused by small reflections in the optical system. Instrument B shows a small, horizontal stripe across the centre of the image. This section of the background has slightly less intensity than other regions of background in the image, which is caused by recovery artefacts in the CCD sensor used in the camera. When these images are processed to produce 1D radial functions as described in 10.1 and the resultant nearfield functions in the baseline are carefully examined, two different patterns emerge.

Since instrument A has a baseline which includes small reflections, the baseline is not constant. The flat section within the reflection region is also between the default averaging radii of 1,15 to 1,2 times the nominal core radius, as shown by the vertical dotted lines (see Figure A.3 below). The baseline near the core includes the additive effect of the reflections; these reflections extend into the image of the core, and so the best estimate of the baseline should include these reflections. If averaging occurred beyond the default averaging radii, the baseline would be biased downward.
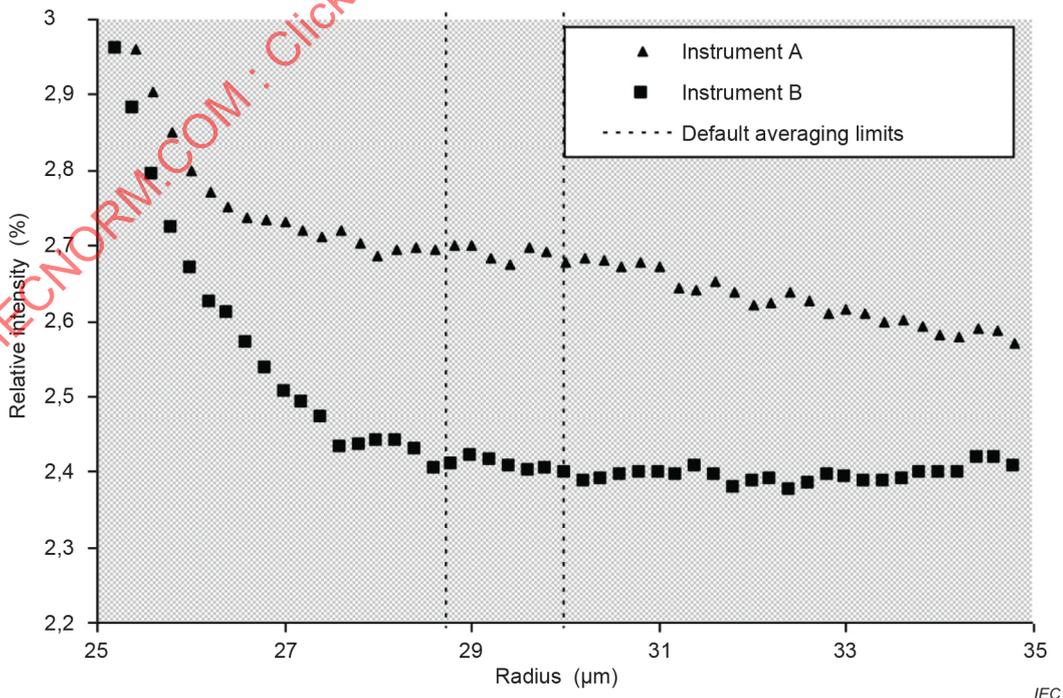

Figure A.3 – Intensity versus radius for instruments A and B

Instrument B has very small modulations in the baseline, and the baseline can be determined by averaging the entire set of data beyond the integration limit of 1,15 times the nominal core radius, thus reducing noise in its estimate.

A.2   Pixel sensitivity variation calibration

Perform the following procedure to determine the pixel sensitivity variation correction matrix $U_{\text{r,c}}$. Record the image, I_{uRaw}, on the detector when it is uniformly illuminated (to within 1 %) with the signal reaching about 75 % of the saturation level (the inside of a small integrating sphere works well as a uniformly illuminated area). Next, record the dark image, I_{uDark}, when the uniform source is off. Compute the average pixel, P_{uAvg}, as shown in Formula (A.1).

$$P_{\text{uAvg}} = \frac{\sum_{r=1}^{N_{\text{r}}} \sum_{c=1}^{N_{\text{c}}} \left(I_{\text{uRaw}_{\text{r,c}}} - I_{\text{uDark}_{\text{r,c}}} \right)}{N_{\text{r}} N_{\text{c}}} \tag{A.1}$$

Compute each element in $U_{\text{r,c}}$ as shown in Formula (A.2).

$$U_{\text{r,c}} = \frac{P_{\text{uAvg}}}{I_{\text{uRaw}_{\text{r,c}}} - I_{\text{uDark}_{\text{r,c}}}} \tag{A.2}$$

The resulting element values will typically range from 0,90 to 1,10. They are to be multiplied by their corresponding pixels, so as to normalize those pixels to the average sensitivity of all pixels, for every measurement that is made.

A.3   Correlated double sampling

One can use "correlated double sampling" (CDS) to almost completely eliminate CCD camera offsets, and their temperature sensitivity, at the cost of some added equipment complexity. Correlated double sampling is also quite effective against uncorrelated stray light. Makers of specialized instruments intended to perform the measurements described in this document would be well advised to implement correlated double sampling.

To implement CDS, one blinks the laser or incoherent calibration source at a frequency somewhere between 5 Hz and 60 Hz, and electrically synchronizes the camera to the periodic blinking in such a way that odd frames are dark (source off), while the even frames see the nearfield to be measured (source on). The odd frames are subsequently subtracted from the preceding even frames, pixel for pixel, yielding an offset-corrected 2D nearfield flux distribution. For best calibration, the "on" time should exactly equal the "off" time. If a series of frames is to be averaged, then all even frames should be added, all odd frames should be subtracted from the sum of even frames, and the resulting difference should be divided by the number of even frames. CDS would replace the entire offset correction scheme in 9.2.3, but pixel sensitivity correction will still be required. If many measurements are to be made, like in a factory, this approach can be a time saver, as many sources of inaccuracy that would otherwise require time and care to correct manually are simply eliminated. The blink rate should be chosen to be an exact sub-multiple of the local power-line frequency, 50 Hz or 60 Hz, to ensure maximum discrimination against artificial stray light and electrical noise, so that an integral number of power frequency sine waves will fit in the time that the source is either on or off. For example, with 60-Hz power, the "on" time and "off" time could both be 1/30 of a second (two complete cycles fit in the on period, and another two complete cycles fit in the off period), yielding a blink

rate of 15 Hz. It is not necessary to phase lock the sampling period to the power-line cycle period; it is sufficient that the sampling period be an exact multiple of the power-line cycle period.

A.4   Imperfections of practical detectors and optics

Cameras vary in their mechanical construction, age, condition, and state of adjustment. Some will contain two-dimensional detectors, where the distortions will be due largely to optics and non-square pixels. Some will mechanically scan a one-dimensional (linesman) CCD more or less perpendicular to its line of pixels. Some will mechanically scan a single pixel (a pinhole) in two dimensions. Others will scan a set of perhaps orthogonal slits over a single large-area detector. Imperfections in these mechanical scanners will cause the X-direction and Y-direction magnification to differ significantly, and non-perpendicular movement of the various mechanical components can also cause shearing (where motion along one axis causes apparent motion in another axis). The camera body (or the CCD chip within) can be slightly rotated about the camera's Z (optical) axis, and the camera can also be slightly tilted with respect to the test jumper assembly's optical axis.

In mathematical terms, all of these geometric distortions can together be expressed as a single overall "affine transformation" between "true space" (micro positioner coordinates) at the fibre face and the "TV space" reported by the camera. Affine transforms are easily expressed with matrices. In practice, one measures the camera's distortions, derives the affine transform, and uses the transform to mathematically compensate subsequent measurements for the camera's geometric distortions. No two cameras will be exactly alike, so this compensation shall be done on a per camera basis (i.e., by serial number). In general, if a camera is working well, it is better to calibrate and compensate mathematically than to try to physically adjust the camera. However, in any case, one shall recalibrate whenever the camera is repaired or adjusted, or the mounting of components to the optical bench or optical plate is disturbed.

Dark current, which is caused by various kinds of electrical leakage within the photodiodes of the CCD chip at the heart of the camera, is a very sensitive function of temperature, typically doubling for each seven degrees centigrade rise in chip temperature. No two pixels (or CCDs) will have exactly the same dark current. Because dark current is integrated during each exposure period, the output voltage offset induced by dark current will vary in direct proportion to exposure duration (integration time).

Fixed-pattern noise, which is due to capacitive feedthrough of logic clock signals into video lines within the CCD chip, has a repetitive and usually complex pattern that does not vary significantly with temperature, illumination, or exposure duration. The pattern is fixed from pixel to pixel; any given pixel will have a substantially constant value.

Pixel crosstalk noise, which is caused by imperfect charge transfer from pixel to pixel as the image is being shifted to the output, causes smearing of the image and bleeding into background areas.

Under reasonable laboratory conditions, the offsets introduced by dark current and fixed-pattern noise combined with pixel crosstalk are typically no more than about 5 % or 10 % of saturation, if stray light has been fully eliminated and the exposure duration is short enough for the temperature.

Pixel sensitivity variation is an effect where the sensitivity (responsivity) of individual pixels to light varies by up to ±10 % from the mean due to manufacturing variations, but does not vary significantly with temperature, illumination, or exposure duration, so long as both saturation ceiling and noise floor are avoided.

Bad pixels are pixels that have little sensitivity to light, remaining stuck at some high or low value, or being very much less sensitive to light than average. Because even 100 bad pixels out of the 30 000 active pixels in a 256 x 256 picture have negligible effect on the results, one

can simply ignore bad pixels in the procedures described in this document, except when determining the centroid threshold, making no attempt to eliminate or compensate for bad pixels.

The above paragraphs discussed the imperfections of the imager chip itself. However, the optical system containing the imager has imperfections as well, in addition to the mechanical misalignments that are calibrated out in Clause 8. For the purposes of this document, the principal imperfections are caused by internal reflections in the optical system, especially reflections within and between the microscope objective and the detector. Reflections can be produced at any optical discontinuity, but especially at air/glass interfaces. These interfaces can be found at the outer surfaces of the magnifying optics, attenuators and filters, beam splitters and the window of the detector package that protects the imager chip. It is possible to use windowless detector packages; this practice can expose the imager chip to the environment causing reliability problems. The degree to which these reflections affect the measurement of encircled flux depends on the location of the reflections within the image, the reflection's intensity, and the shape of the reflection.

The useful way to tell if a spot in an image is caused by a reflection is to move the fibre end-face (input port) in the XY plane, and observe the resulting motion of the spots. Reflections will generally move along the line of fibre end-face motion, but at a greater or lesser speed than the direct image of the fibre end-face, and often in the opposite direction. Compressing and false-colouring these images, as demonstrated in Figure A.2, can help in detecting these reflections.

The most common remedy is the use of anti-reflection coatings on all optical surfaces, and this works reasonably well if the test wavelength is well matched to the wavelength range for which the coating was designed.

In addition, one can arrange the optical system such that reflections fall into harmless locations. The simplest way to accomplish this is to move the centre of the fibre face to one side of the microscope objective's optical axis and the centre of the imager chip to the other side, while maintaining the various planes (image, object, and principal) in parallel, depending on the flat field of the objective to maintain focus despite these displacements. Then, light from the objective will arrive at an angle to the window, and will be reflected off to one side.

The parallel-displacement approach mentioned above is a special case of the "Scheimpflug condition", which is the principle behind view cameras in photography. The Scheimpflug condition is met when the image plane, the object plane, and the corresponding lens principal planes all intersect the same line. This intersection line will be well away from the image or object, and in the case of parallel displacement, will be at infinity.

When the Scheimpflug condition is met, the image will be in perfect focus despite the tilted image, lens, and object planes. With parallel planes, the magnification factors do not depend on location in the image; while with intersecting planes, the magnification factors will vary linearly with location in the image. This varying magnification factor is easily handled using projective geometry, but the considerable added complexity did not seem justified, as the parallel planes and affine geometry of this document approach are adequate.

Bibliography

IEC 60793-1-20 , *Optical fibres – Part 1-20: Measurement methods and test procedures – Fibre geometry*

IEC 60793-1-41, *Optical fibres – Part 1-41: Measurement methods and test procedures – Bandwidth*

IEC 61745:2017, *End-face image analysis procedure for the calibration of optical fibre geometry test sets*

ANSI/EIA-440-B:2004, *Fiber optic terminology*

David F. Rogers and J. Alan Adams, *Mathematical elements for computer graphics*, 2nd edition, McGraw-Hill, 1990

James R. Janesick, *Scientific charge-coupled devices*, SPIE Press, 2001

James R. Janesick, Morely M. Blouke, and J. Freeman, *Scientific charge-coupled devices*, Optical Engineering, August 1987, Vol. 26, No. 8, pp. 692-714

Foley et al, Addison-Wesley, *Computer graphics: principles and practice*, 2nd edition, 1990

Holst, Gerald C., *Electro-optical imaging system performance*, JCD Publishing and SPIE Press, 1995

_____

SOMMAIRE

COMMISSION ÉLECTROTECHNIQUE INTERNATIONALE

_____

PROCÉDURES D'ESSAI DES SOUS-SYSTÈMES DE TÉLÉCOMMUNICATION FIBRONIQUES –

Partie 1-4: Sous-systèmes généraux de télécommunication – Méthode de mesure du flux inscrit de la source optique

AVANT-PROPOS

1) La Commission Electrotechnique Internationale (IEC) est une organisation mondiale de normalisation composée de l'ensemble des comités électrotechniques nationaux (Comités nationaux de l'IEC). L'IEC a pour objet de favoriser la coopération internationale pour toutes les questions de normalisation dans les domaines de l'électricité et de l'électronique. A cet effet, l'IEC – entre autres activités – publie des Normes internationales, des Spécifications techniques, des Rapports techniques, des Spécifications accessibles au public (PAS) et des Guides (ci-après dénommés "Publication(s) de l'IEC"). Leur élaboration est confiée à des comités d'études, aux travaux desquels tout Comité national intéressé par le sujet traité peut participer. Les organisations internationales, gouvernementales et non gouvernementales, en liaison avec l'IEC, participent également aux travaux. L'IEC collabore étroitement avec l'Organisation Internationale de Normalisation (ISO), selon des conditions fixées par accord entre les deux organisations.

2) Les décisions ou accords officiels de l'IEC concernant les questions techniques représentent, dans la mesure du possible, un accord international sur les sujets étudiés, étant donné que les Comités nationaux de l'IEC intéressés sont représentés dans chaque comité d'études.

3) Les Publications de l'IEC se présentent sous la forme de recommandations internationales et sont agréées comme telles par les Comités nationaux de l'IEC. Tous les efforts raisonnables sont entrepris afin que l'IEC s'assure de l'exactitude du contenu technique de ses Publications; l'IEC ne peut pas être tenue responsable de l'éventuelle mauvaise utilisation ou interprétation qui en est faite par un quelconque utilisateur final.

4) Dans le but d'encourager l'uniformité internationale, les Comités nationaux de l'IEC s'engagent, dans toute la mesure possible, à appliquer de façon transparente les Publications de l'IEC dans leurs publications nationales et régionales. Toutes divergences entre toutes Publications de l'IEC et toutes publications nationales ou régionales correspondantes doivent être indiquées en termes clairs dans ces dernières.

5) L'IEC elle-même ne fournit aucune attestation de conformité. Des organismes de certification indépendants fournissent des services d'évaluation de conformité et, dans certains secteurs, accèdent aux marques de conformité de l'IEC. L'IEC n'est responsable d'aucun des services effectués par les organismes de certification indépendants.

6) Tous les utilisateurs doivent s'assurer qu'ils sont en possession de la dernière édition de cette publication.

7) Aucune responsabilité ne doit être imputée à l'IEC, à ses administrateurs, employés, auxiliaires ou mandataires, y compris ses experts particuliers et les membres de ses comités d'études et des Comités nationaux de l'IEC, pour tout préjudice causé en cas de dommages corporels et matériels, ou de tout autre dommage de quelque nature que ce soit, directe ou indirecte, ou pour supporter les coûts (y compris les frais de justice) et les dépenses découlant de la publication ou de l'utilisation de cette Publication de l'IEC ou de toute autre Publication de l'IEC, ou au crédit qui lui est accordé.

8) L'attention est attirée sur les références normatives citées dans cette publication. L'utilisation de publications référencées est obligatoire pour une application correcte de la présente publication.

9) L'attention est attirée sur le fait que certains des éléments de la présente Publication de l'IEC peuvent faire l'objet de droits de brevet. L'IEC ne saurait être tenue pour responsable de ne pas avoir identifié de tels droits de brevets.

L'IEC 61280-1-4 a été établie par le sous-comité 86C: Systèmes et dispositifs actifs à fibres optiques, du comité d'études 86 de l'IEC: Fibres optiques. Il s'agit d'une Norme internationale.

Cette troisième édition annule et remplace la deuxième édition parue en 2009. Cette édition constitue une révision technique.

Cette édition inclut les modifications techniques majeures suivantes par rapport à l'édition précédente:

a) amélioration de la procédure et de la traçabilité de l'étalonnage;

b) amélioration de la description et des exigences relatives à l'agitateur de fibre;

c) ajout des sources optiques pulsées;

d) suppression d'un processus d'étalonnage utilisant un micropositionneur, en raison de sa faible traçabilité.

Le texte de cette Norme internationale est issu des documents suivants:

Projet	Rapport de vote
86C/1806/CDV	86C/1828/RVC

Le rapport de vote indiqué dans le tableau ci-dessus donne toute information sur le vote ayant abouti à son approbation.

La langue employée pour l'élaboration de cette Norme internationale est l'anglais.

Ce document a été rédigé selon les Directives ISO/IEC, Partie 2, il a été développé selon les Directives ISO/IEC, Partie 1 et les Directives ISO/IEC, Supplément IEC, disponibles sous www.iec.ch/members_experts/refdocs. Les principaux types de documents développés par l'IEC sont décrits plus en détail sous www.iec.ch/publications.

Une liste de toutes les parties de la série IEC 61280, publiées sous le titre général *Procédures d'essai des sous-systèmes de télécommunication fibroniques*, se trouve sur le site web de l'IEC.

Le comité a décidé que le contenu de ce document ne sera pas modifié avant la date de stabilité indiquée sur le site web de l'IEC sous webstore.iec.ch dans les données relatives au document recherché. A cette date, le document sera

- reconduit,
- supprimé,
- remplacé par une édition révisée, ou
- amendé.

IMPORTANT – Le logo "colour inside" qui se trouve sur la page de couverture de ce document indique qu'elle contient des couleurs qui sont considérées comme utiles à une bonne compréhension de son contenu. Les utilisateurs devraient, par conséquent, imprimer cette publication en utilisant une imprimante couleur.

INTRODUCTION

La présente partie de l'IEC 61280 spécifie comment mesurer le flux inscrit d'une source optique multimodale. Le flux inscrit est une fraction de la puissance de sortie cumulée sur la puissance de sortie totale, en fonction de la distance radiale depuis le centre du cœur de la fibre optique multimodale.

L'approche de base consiste à rassembler des données de champ proche bidimensionnelles (2D) en utilisant une caméra étalonnée, et à convertir mathématiquement ces données en 2D en trois fonctions normalisées de la distance radiale par rapport au centre optique de la fibre. Les trois fonctions sont l'intensité, le flux incrémental et le flux inscrit. L'intensité représente la puissance optique par zone (exprimée en watts par mètre carré). Le flux incrémental représente la puissance optique par différentiel de rayon (exprimée en watts par mètre), et le flux inscrit représente une fraction de la puissance de sortie cumulée sur la puissance de sortie totale.

Ces trois fonctions radiales sont destinées à caractériser des sources laser fibroniques utilisées dans des modèles mathématiques prévoyant la longueur garantie minimale d'une liaison de communication, ou pour qualifier une source optique afin de mesurer la perte d'insertion dans des liaisons multimodales.

**PROCÉDURES D'ESSAI DES SOUS-SYSTÈMES
DE TÉLÉCOMMUNICATION FIBRONIQUES –**

**Partie 1-4: Sous-systèmes généraux de télécommunication –
Méthode de mesure du flux inscrit de la source optique**

1 Domaine d'application

La présente partie de l'IEC 61280 stipule le processus de caractérisation de la méthode de mesure du flux inscrit de sources optiques destinées à être utilisées avec des fibres multimodales.

Le présent document définit une procédure consistant à collecter des données fibroniques de champ proche, bidimensionnelles et en niveaux de gris, puis à les réduire en données unidimensionnelles exprimées sous la forme d'un ensemble de trois fonctions paramétriques échantillonnées du rayon par rapport au centre optique de la fibre.

L'évaluation du diamètre du cœur des fibres ne constitue pas un objectif du présent document.

2 Références normatives

Les documents suivants sont cités dans le texte de sorte qu'ils constituent, pour tout ou partie de leur contenu, des exigences du présent document. Pour les références datées, seule l'édition citée s'applique. Pour les références non datées, la dernière édition du document de référence s'applique (y compris les éventuels amendements).

IEC 60793-2-10, *Fibres optiques – Partie 2-10: Spécifications de produits – Spécification intermédiaire pour les fibres multimodales de catégorie A1*

IEC 60825-1, *Sécurité des appareils à laser – Partie 1: Classification des matériels et exigences*

3 Termes et définitions

Pour les besoins du présent document, les termes et définitions suivants s'appliquent.

L'ISO et l'IEC tiennent à jour des bases de données terminologiques destinées à être utilisées en normalisation, consultables aux adresses suivantes:

- IEC Electropedia: disponible à l'adresse https://www.electropedia.org/
- ISO Online browsing platform: disponible à l'adresse https://www.iso.org/obp

**3.1
source optique d'étalonnage**
source optique utilisée pour déterminer le centre optique d'une fibre multimodale

**3.2
image du centroïde**
image utilisée pour déterminer le centre optique du cœur de la fibre multimodale

3.3
image corrigée
image à partir de laquelle une image d'obscurité a été soustraite et dont les éléments ont subi une correction d'uniformité

3.4
image d'obscurité
image prise avec la source optique mesurée éteinte ou non installée sur le port d'entrée

Note 1 à l'article: La lumière parasite et les signaux électriques du système de détection restent dans l'image d'obscurité.

3.5
image
matrice rectangulaire bidimensionnelle de nombres dont les éléments sont des pixels et dont les valeurs des pixels correspondent linéairement à la puissance optique atteignant les pixels

3.6
source optique
dispositif qui émet un rayonnement lumineux, couplé à une fibre, dont la sortie peut être mesurée

EXEMPLE   Source optique d'étalonnage, source optique de transmission ou source optique utilisée dans le cadre de mesures d'affaiblissement.

3.7
source optique de mesure
source optique destinée à être utilisée dans le cadre de la mesure de l'affaiblissement

3.8
rayon nominal du cœur
moitié du diamètre nominal du cœur de la fibre multimodale à mesurer

3.9
lissage en anneau
technique permettant de réduire l'image du champ proche bidimensionnel en un profil d'intensité de champ proche unidimensionnel tout en supprimant les effets de l'espacement périodique des pixels de l'imageur de surface finie

3.10
source optique de transmission
source optique utilisée pour transmettre des données numériques sur des liaisons fibroniques multimodales

3.11
correction d'uniformité
processus permettant de corriger la sensibilité d'un pixel de telle sorte qu'il se comporte essentiellement comme un pixel moyen

3.12
pixel valide
élément de détection optique dans la matrice du détecteur dont la sensibilité, lorsqu'elle est corrigée, est comprise dans une gamme de 5 % autour de la sensibilité moyenne du rendement de conversion du détecteur

4 Symboles

B	intensité de la ligne de base

NOTE 1   Cette valeur est déterminée à partir d'une région du champ proche calculé situé juste à l'extérieur du bord du cœur.

D	distance entre le centre de l'image du centroïde et le bord le plus proche de l'image
D_L, D_R, D_T, D_B	ensemble des distances entre le centre de l'image du centroïde et, respectivement, le bord gauche, droit, haut et bas de l'image

NOTE 2   Le minimum de cet ensemble est utilisé pour calculer D.

$EF(i)$	vecteur du flux inscrit
$EF'(i)$	vecteur du flux inscrit non normalisé
i	paramètre d'indice utilisé dans les vecteurs de résultats paramétriques et $EF(i)$
I_{dark}	matrice des intensités des pixels d'une image d'obscurité telles qu'elles sont mesurées par le détecteur et le numériseur
I_{raw}	matrice des intensités des pixels de la source optique, avant correction, telles qu'elles sont mesurées par le détecteur et le numériseur d'images
$I_{r,c}$	matrice des intensités du champ proche

NOTE 3   Il s'agit d'une matrice des intensités des pixels, basée sur I_{raw}, telles qu'elles sont mesurées par le détecteur et corrigées à l'aide de U et I_{dark}.

$I(i)$	vecteur d'intensité du lissage en anneau, chaque élément étant la moyenne arithmétique de l'ensemble des coordonnées radiales de tous les pixels dans un anneau donné
N_R	nombre d'anneaux utilisés pour calculer le champ proche unidimensionnel
N_r	nombre de lignes dans une image

NOTE 4   Toutes les colonnes dans une image ont le même nombre de lignes.

N_c	nombre de colonnes dans une image

NOTE 5   Toutes les lignes dans une image ont le même nombre de colonnes.

P_{Max}	pixel valide le plus intense dans l'image du centroïde
P_{Min}	pixel valide le moins intense dans l'image du centroïde
R	coordonnées radiales, en µm, du centre de n'importe quel pixel, référencées par rapport au centre optique X_0, Y_0
$R(i)$	vecteur radial du lissage en anneau, chaque élément étant la moyenne arithmétique des rayons de tous les pixels dans le $i^{ème}$ anneau
R_{max}	limite d'intégration le long du rayon
S_c	somme pondérée sur les colonnes de toutes les intensités des pixels supérieurs à T dans l'image du centroïde
$S_I(i)$	vecteur de la somme des intensités utilisé pour le lissage en anneau
S_P	somme de toutes les intensités des pixels supérieures à T dans l'image du centroïde
$S_N(i)$	vecteur de comptage des pixels utilisé pour le lissage en anneau
$S_R(i)$	vecteur de la somme des rayons utilisé pour le lissage en anneau

S_r	somme pondérée sur les lignes de toutes les intensités des pixels supérieures à T dans l'image du centroïde
S_x	facteur d'étalonnage géométrique horizontal (le long des colonnes)
S_Y	facteur d'étalonnage géométrique vertical (le long des lignes)
T	seuil utilisé pour déterminer quels pixels dans l'image du centroïde sont utilisés pour déterminer le centre optique

NOTE 6   Tous les pixels supérieurs ou égaux à T sont utilisés pour calculer le centroïde.

$U_{r,c}$	matrice de correction de la sensibilité, appliquée à une image à partir de laquelle une image d'obscurité a été soustraite, afin de réduire la non-uniformité du rendement de conversion du détecteur, pixel par pixel
W	demi-largeur, en µm, des anneaux utilisés pour calculer le champ proche unidimensionnel
X_0	emplacement sur l'axe X (colonnes) du centre de l'image du centroïde
Y_0	emplacement sur l'axe Y (lignes) du centre de l'image du centroïde

5   Hypothèses

5.1   Hypothèses applicables à la caractérisation des sources de données

La fibre multimodale à gradient d'indice quasi parabolique à cœur de 50 µm ou 62,5 µm, utilisée comme "ensemble jarretière d'essai", est traitée comme si elle présentait une symétrie circulaire parfaite autour de son centre optique. En effet, les asymétries dans les distributions de flux optiques injectées l'emportent sur toute distorsion induite par l'ensemble jarretière d'essai, telle que les désalignements latéraux et angulaires. Il est en outre présumé que tous les modes de gaine sont extraits en traversant les 10 m ou plus spécifiés de fibre. Les modes d'un groupe de modes peuvent ne pas transporter un flux égal. En fait, avec de telles fibres courtes, de 1 000 m ou moins, une distribution inégale du flux dans les modes d'un groupe constitue la norme, et non l'exception.

### 5.2   Hypothèses applicables à la caractérisation des sources de mesure

Il est présumé que les sources de mesure disposent d'une bande suffisamment large et qu'elles présentent une incohérence suffisante pour que la tacheture ne constitue pas un problème. Il est en outre présumé que la distribution du champ proche est suffisamment symétrique pour que le centroïde tronqué de ce champ proche indique l'emplacement du centre optique de la fibre avec une précision suffisante pour atteindre les objectifs du présent document.

6   Appareillage

6.1   Appareillage commun

6.1.1   Généralités

La Figure 1 ci-dessous représente le schéma fonctionnel de l'appareillage.
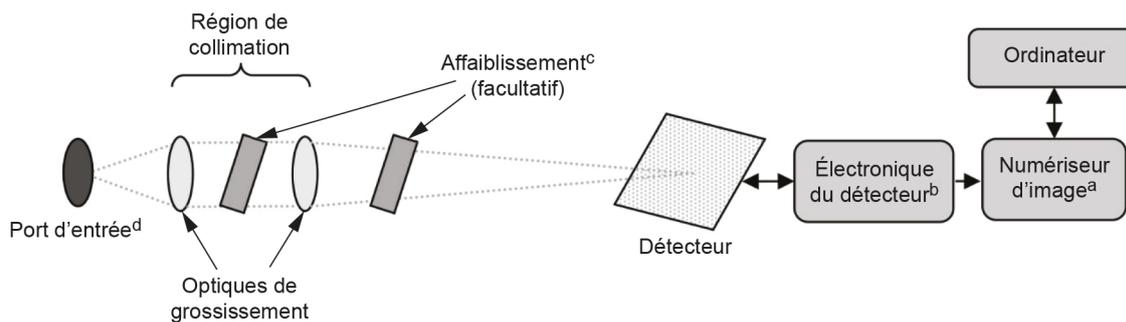
IEC

a Le numériseur d'images peut soit faire partie d'une caméra, soit être une carte d'extension dans un ordinateur.

b L'électronique du détecteur est généralement intégrée à la caméra et au numériseur.

c Idéalement, l'affaiblissement est placé dans la région de collimation du trajet optique, mais les architectures optiques ne présentent pas toutes une région de collimation accessible. Dans ce cas, il convient de placer l'affaiblissement du côté détecteur, par rapport aux optiques.

d Lorsqu'un micropositionneur (non représenté) est utilisé, le port d'entrée est rattaché physiquement à celui-ci.

Figure 1 – Schéma fonctionnel de l'appareillage

6.1.2 Ordinateur

Un ordinateur est exigé car l'image acquise contient des milliers de pixels et la réduction de l'image au flux inscrit exige une capacité de calcul substantielle. L'ordinateur est généralement connecté au numériseur d'images pour commander l'acquisition d'une image par l'intermédiaire d'un logiciel, et il peut également commander le micropositionneur (et la source, si un double échantillonnage corrélé est mis en œuvre).

6.1.3 Numériseur d'image

Une image du champ proche du cœur de la fibre est créée sur le détecteur, puis numérisée par le numériseur d'image. Le numériseur d'image peut faire partie intégrante d'une caméra, qui contient également le détecteur, ou il peut s'agir d'une carte d'extension de capture de trames, au sein de l'ordinateur.

Les circuits automatiques du numériseur, par exemple une commande automatique de gain, que l'on trouve souvent dans les caméras vidéo, doivent être désactivés.

6.1.4 Détecteur

Le détecteur est typiquement une caméra à dispositif à couplage de charge (CCD, Charge-Coupled Device) ou à semiconducteur à oxyde métallique complémentaire (CMOS, Complementary Metal-Oxide Semiconductor). D'autres types de caméras matricielles peuvent être pris en compte. Dans tous les cas, les détecteurs doivent être à la fois linéaires et sans effet mémoire. Une mesure radiométrique absolue du flux (puissance du flux optique) n'est pas exigée.

Les circuits automatiques du détecteur, par exemple une commande automatique de gain, que l'on trouve souvent dans les caméras vidéo, doivent être désactivés.

La différence de sensibilité de conversion d'un pixel à un autre dans le détecteur affecte la précision de mesure. La non-uniformité du rendement de conversion corrigé du détecteur ne doit pas dépasser ±5 %. Il est possible d'étalonner et de corriger le détecteur dont la non-uniformité non corrigée est supérieure à 5 % en appliquant une matrice de correction de la sensibilité pixel par pixel, U, à l'image brute. Souvent, cette correction fait partie des fonctions de la caméra (et donc chaque élément de U peut être considéré comme unitaire). Parfois, la matrice de correction peut être fournie par le fournisseur du détecteur. Dans les autres cas, la matrice de correction doit être déterminée par la procédure décrite à l'Article A.2.

Les détecteurs peuvent avoir des pixels invalides, qui sont des pixels dont le rendement de conversion corrigé dépasse ±5 % du rendement de conversion moyen du détecteur. Les pixels invalides ne produisent souvent aucun signal, un signal complètement saturé, ou sont bloqués à une valeur intermédiaire. Les détecteurs dont le nombre de pixels invalides dépasse 0,1 % du nombre total de pixels doivent être rejetés.

Dans la plupart des caméras et des numériseurs d'image, le réglage du "niveau de noir" peut être ajusté par l'utilisateur. Puisque le détecteur sera légèrement bruité, il est important que le détecteur et le numériseur n'écrêtent pas les signaux de noir aléatoires à zéro (dans les systèmes habituels, le bruit aléatoire dans un détecteur présente un écart-type inférieur à 0,5 % du niveau de saturation). Pour assurer l'absence d'écrêtage du bruit, lorsque celui-ci est réglable, le niveau de noir est à régler afin de produire un petit signal positif (typiquement au moins cinq fois l'écart-type du bruit) lorsqu'aucune lumière n'atteint le détecteur.

6.1.5 Optiques de grossissement

Des optiques appropriées doivent être prévues pour projeter une image agrandie du port d'entrée sur le détecteur de telle sorte que le détecteur puisse mesurer toute la distribution du flux du champ proche. L'ouverture numérique des optiques de grossissement doit dépasser l'ouverture numérique nominale des fibres (comme cela est indiqué dans la spécification de la famille de fibres) utilisée pour l'étalonnage ou les mesures. Les objectifs des microscopes répondent souvent à cette exigence.

NOTE   Lorsque l'objectif d'un microscope est utilisé, son grossissement réel tel qu'il est utilisé dans l'appareillage n'est généralement pas le même que le facteur de grossissement nominal gravé sur le côté de l'objectif. Ceci parce que l'appareillage est différent du microscope normal pour lequel le facteur de grossissement nominal a été calculé. Les procédures d'étalonnage géométrique présentées dans l'Article 8 déterminent le grossissement réel.

Les réflexions à partir des surfaces optiques peuvent sérieusement dégrader la mesure du flux inscrit. Un revêtement antiréflexion à la longueur d'onde de la mesure, ou d'autres formes de contrôle des réflexions, peuvent-être considérés pour réduire les réflexions.

La précision de mesure est importante lors de la caractérisation des sources optiques de mesure, de sorte que la distorsion optique soit maintenue à un niveau minimal. Il est recommandé de choisir et d'utiliser avec soin les lentilles et les autres composants optiques. Les objectifs de microscopes de type plan constituent un exemple d'optiques appropriées. Les procédures présentées dans l'IEC 61745:2017 peuvent être utilisées pour évaluer l'intégrité optique de l'appareillage.

Il est important que la distance entre le détecteur et tous les éléments des optiques de grossissement ne soit pas modifiée après l'étalonnage. Lorsque la distance entre ces éléments change, le grossissement est susceptible d'être modifié dans des proportions suffisantes pour qu'un nouvel étalonnage soit exigé. La focalisation doit être effectuée en modifiant uniquement la distance entre le port d'entrée et les optiques de grossissement.

6.1.6 Atténuateur

Souvent, le flux optique de la source sature le détecteur et la seule solution efficace consiste à utiliser un atténuateur optique. Dans tous les cas, l'atténuateur ne doit pas réduire l'ouverture numérique du système optique et ne doit pas être la source de réflexions ni de distorsions optiques importantes, qui introduiraient un biais sur le flux inscrit résultant.

NOTE 1   Lorsque des filtres de densité neutre sont utilisés dans le système optique, des distorsions géométriques peuvent apparaître.

NOTE 2   Le fait de modifier l'affaiblissement entre l'image du centre optique et l'image de la source mesurée peut éloigner l'emplacement du centre optique de la source de mesure par rapport à l'emplacement qui a été déterminé en utilisant l'image du centre optique. Ceci entraîne des erreurs dans les fonctions des données radiales résultantes.

6.1.7   Micropositionneur (facultatif)

Le micropositionneur est une partie optionnelle de l'appareillage. En fonction de la conception de l'appareillage, il est possible de se servir de la géométrie de la férule du connecteur pour placer toute l'image sur le détecteur sans utiliser de micropositionneur. Dans de nombreuses mises en œuvre, seul un réglage du foyer (axe Z) est nécessaire. Dans certains cas, les trois axes peuvent n'exiger un alignement que lors de la construction ou de la maintenance de l'appareillage. L'utilisation de la férule pour placer l'image du cœur de la fibre sur le détecteur ne dispense pas de l'exigence d'identification du centre optique, comme cela est exigé par 9.3.

Le but du micropositionneur est de focaliser l'image projetée de la face de la fibre sur le détecteur et de déterminer le grossissement de l'appareillage (voir Article 8). Des mécanismes de verrouillage mécaniques ou des mécanismes équivalents sont exigés sur les trois axes afin d'éviter une dérive mécanique pendant les mesures. Le micropositionneur peut facultativement être entraîné par des moteurs et peut facultativement utiliser des mécanismes de rétroaction pour commander la position réelle de l'étage (et donc de la face de la fibre).

6.1.8   Port d'entrée

Le port d'entrée est l'endroit où les artefacts d'étalonnage et les échantillons de mesure sont connectés à l'appareillage. Les caractéristiques du port d'entrée dépendent du type de source à caractériser.

Lors de la caractérisation de sources optiques de transmission, le port d'entrée est l'extrémité distale de l'ensemble jarretière d'essai. L'extrémité proximale de l'ensemble jarretière d'essai est représentée sur le détecteur. Lorsqu'un micropositionneur est utilisé, l'extrémité proximale est fixée au micropositionneur.

Lors de la caractérisation de sources optiques de mesure, le port d'entrée est généralement la platine du connecteur, ou son équivalent. Lorsqu'un micropositionneur est utilisé, la platine est fixée au micropositionneur.

Les exigences particulières sont présentées en 6.2 et 6.3.

6.1.9   Source optique d'étalonnage

La source optique d'étalonnage est utilisée pour étalonner l'appareillage (voir Article 8). Lorsque cette source est utilisée pour éclairer l'ensemble jarretière d'essai, la source d'étalonnage doit saturer les modes de la jarretière. Un embrouilleur de modes peut facultativement être utilisé avec la source d'étalonnage choisie afin d'assurer une saturation modale plus uniforme de la fibre. Voir l'IEC 60793-1-41 pour obtenir des informations sur les embrouilleurs de modes.

Toute source optique non cohérente à large spectre, telle qu'une lampe halogène au tungstène, une lampe à arc au xénon ou une diode électroluminescente (LED), peut être utilisée pour saturer la distribution modale de la fibre de l'ensemble jarretière d'essai. Lors de l'étalonnage de l'appareillage pour la caractérisation des sources optiques de mesure, la longueur d'onde centrale de la source d'étalonnage doit être à moins de 30 nm de la longueur d'onde nominale des sources optiques à qualifier, et sa largeur spectrale (c'est-à-dire largeur totale à mi-maximum) ne doit pas dépasser 100 nm. Lors de l'étalonnage de l'appareillage pour la caractérisation des sources optiques de transmission, les caractéristiques spectrales de la source d'étalonnage ne sont pas spécifiées, mais il est recommandé que son spectre soit similaire aux sources à caractériser. L'intensité de la source d'étalonnage choisie doit être stable sur une période de temps suffisante pour effectuer les mesures.